large-scale expansion culture to ensure the availability of sufficient amounts of cells. The number of Vγ9Vδ2 Tcells in each injection ranged from 0.6 to 69.8 × 10^8 (median 59.0 × 10^8) (Table 2). The Vγ9Vδ2 T cells from all of the patients displayed good effector function as assessed by their in vitro cytotoxicity against Daudi cells (Table 2).

Activated Vγ9Vδ2 T cells exert antitumor effector activity through TCR and NK receptors such as NKG2D. NK receptors-dependent or Vγ9Vδ2 TCR-dependent recognition of tumor cell was evaluated by CD107 translocation assay using pravastatin- or zoledronate-pretreated Daudi cells (Fig. 2). When the baseline tumor cell recognition by NK receptors was evaluated against pravastatin-treated Daudi cells, %$CD107^+$ Vγ9Vδ2 T cells was 55%. The proportion of $CD107^+$ Vγ9Vδ2 T cells against Daudi or z-Daudi cells increased from 63.3% to 96.9% according to the concentration of zoledronate, and reached the plateau at 50 μmol/L or higher. These results were consistent with previous reports that the optimum inhibition of FPP synthase activity was achieved by high zoledronate concentration [30]. The cytotoxic activities of patients' Vγ9Vδ2 T cells against z-Duadi and Daudi cells were summarized in Table S2.

Dynamics of zoledronate and Vγ9Vδ2 T-cells injection

Three patients completed the course of four Vγ9Vδ2 T-cell transfers; patient 2328 received an additional two

Table 2. Adoptively transferred Vγ9Vδ2 T-cells

Patient ID	Cell number (×10^8 cells) (purity of γδ T cells)				Cumulative number of γδ T cell infusions (×10^8 cells)	Average number of γδ T cell infusions (×10^8 cells)	% cytotoxicity against z-Daudi[1] E/T ratio		
	First	Second	Third	Fourth			1:1	5:1	25:1
2305	0.6 (27.6%)				0.6	0.6	18.1	30.3	30.1
2307	58.8 (81.7%)				58.8	58.8	31.4	40.9	53
2319	55.4 (77.0%)	60.5 (84.0%)	65.6 (85.2%)	68.5 (85.6%)	250	62.5	41.3	58	74.6
2325	49.7 (84.3%)	60 (88.3%)	69.8 (89.5%)	40.1 (89.0%)	219.6	54.9	14.2	39.3	60.2
2334	8.6 (71.5%)	45.1 (77.8%)	52.7 (82.3%)		106.4	35.5	45.1	79.7	84.6
2336	64.9 (94.0%)				64.9	64.9	28.9	57	55.4
2328	62.4 (90.4%)	59.2 (92.5%)	65.7 (93.9%)	51.7 (92.3%)	239	59.8	38.3	64.5	72.2

[1]% cytotoxicity against Daudi cells was provided in Table S2.

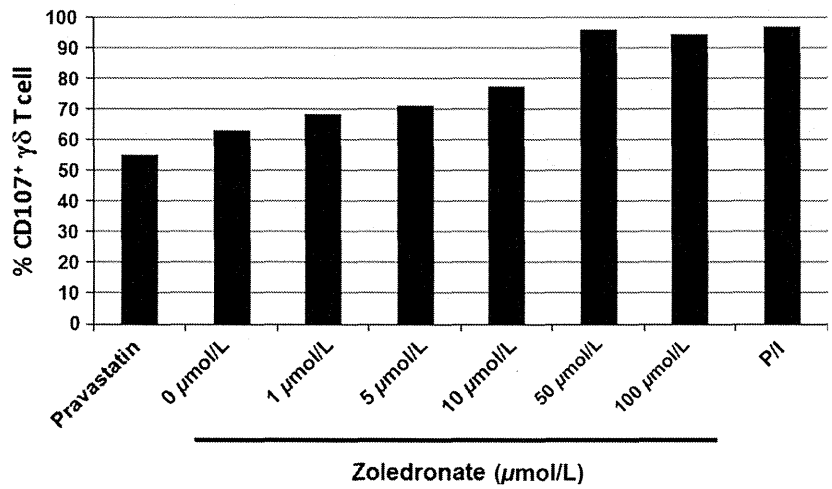

Figure 2. IPP accumulation by zoledronate was evaluated by the CD107 translocation assay of Vγ9Vδ2 T-cells. Daudi cells were preincubated overnight with indicated concentration of zoledronate (0, 1, 5, 10, 50, and 100 μmol/L) or 10 μmol/L pravastatin sodium and used as stimulator cells. The 5 × 10^5 Daudi cells were incubated with the same number of Vγ9Vδ2 T-cells for 2 h at 37°C in the presence of GolgiStop and anti-CD107a/b mAbs. Vγ9Vδ2 T-cells were also stimulated with PMA (20 ng/mL)/ionomycin (2 μg/mL). CD107 translocation was measured by flow cytometry. Results were expressed as percentages of positive cells within the Vγ9Vδ2 T-cell population.

infusions. After each i.p. injection, a large number of Vγ9Vδ2 T cells was observed in the ascites (Fig. 3A); however, Vγ9Vδ2 T cells were not increased in the blood (data not shown), suggesting that they did not enter the systemic circulation from the peritoneal cavity. The number of Vγ9Vδ2 T-cells in ascites rapidly decreased within 7 days except in patient 2319.

It has been reported that zoledronate declines rapidly from the plasma with half-lives of 0.2 h [31]. By systemic injection of zoledronate, the concentration of zoledronate in the ascites might not be sufficient to block the mevalonate pathway and accumulate IPP in the tumor cells. Therefore, we compared the route of zoledronate injection, i.v. or i.p., preceded the infusion of Vγ9Vδ2 T-cell administration. After i.v. zoledronate and i.p. Vγ9Vδ2 T-cell injection, IFN-γ production was detected in patient 2307 and 2328, but not in patients 2305, 2319, 2325, and 2336 (Fig. 3B). Importantly, the IFN-γ production was observed when both zoledronate and Vγ9Vδ2 T cells were i.p. injected. In patient 2334, i.v. zoledronate injection was omitted; she received three courses of i.p. zoledronate injection followed by i.p. Vγ9Vδ2 T-cell injection. IFN-γ was detected in the ascites with each Vγ9Vδ2 T-cell injection.

Consistently, the concentration of zoledronate in the ascites fluid was higher and sustained longer after i.p. zoledronate injection than i.v. injection (Fig. S1). PBMCs from healthy donor were stimulated with indicated amount of zoledronate in AlyS203 medium containing 1000 IU/mL human recombinant IL-2 and 10% pooled human serum. Same donor derived PBMCs were cultured in IL-2 containing medium and in the presence of 10%

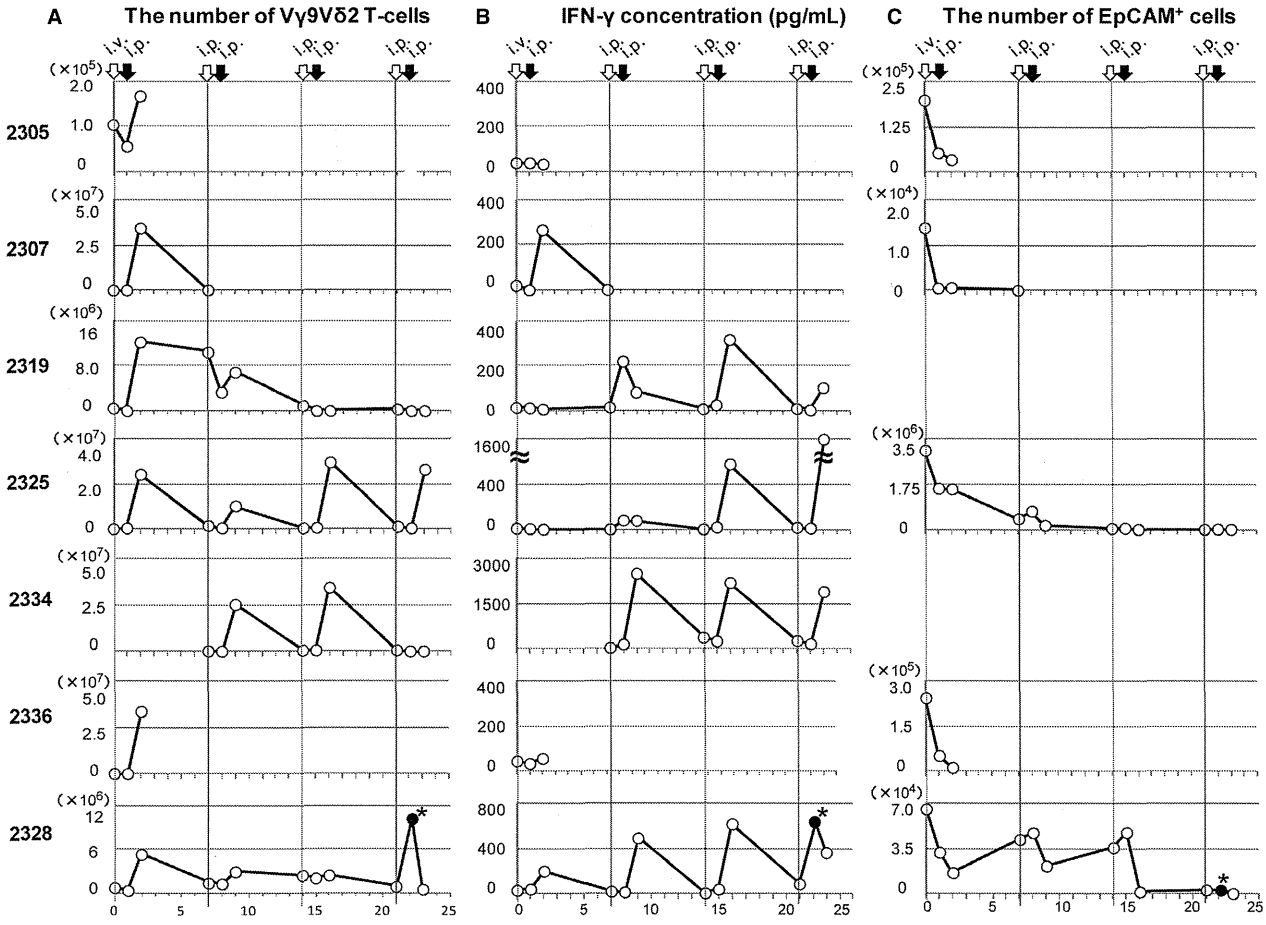

Figure 3. Dynamics of Vγ9Vδ2 T cells and responses in patients with malignant ascites. (A) The number of Vγ9Vδ2 T cells in ascites. The ascites fluid was drained from the peritoneal cavity via the indwelling catheter before zoledronate and Vγ9Vδ2 T-cell injections and 24 h after Vγ9Vδ2 T-cell injections. The cells were isolated by density gradient centrifugation and stained with anti-CD45, -CD3, and -TCRVγ9. The stained cells were analyzed on flow cytometry and the numbers of Vγ9Vδ2 T cells calculated. (B) IFN-γ concentration (pg/mL) in ascites at the indicated time points was measured by the FlowCytomix bead assay. (C) The cells from ascites were also stained with anti-EpCAM mAb and the numbers of EpCAM+ tumor cells calculated. *Sample was collected 4 h after i.p. Vγ9Vδ2 T-cell injection.

patient ascites fluid for 14 days. The concentration of zoledronate was estimated by the expansion of Vγ9Vδ2 T cells. While zoledronate was not detectable in the ascites harvested after i.v. zoledornate injection, the zoledronate concentration in the ascites peaked 34.5 ± 20 nmol/L at 2 h, and rapidly declined to 10 nmol/L within 4 h after i.p. injection. The peak concentration reached higher and zoledronate concentration in the ascites sustained longer when zoledronate was i.p. injected than i.v. injected. These results indicated that local administration of zoledronate is important to sensitize tumor cells to Vγ9Vδ2 T-cell recognition.

The cytotoxicity of Vγ9Vδ2 T cells

Because tumor cells from patients 2319 and 2334 were negative for EpCAM, it was difficult to calculate their precise tumor load. In the other five patients, the number of $EpCAM^+$ tumor cells in ascites fluid were significantly reduced after zoledronate and Vγ9Vδ2 T-cell treatment (Fig. 3C). Immunoflueorscence microscopy revealed that Vγ9Vδ2 T cells attached to and surrounded $EpCAM^+$ tumor cells (Fig. 4A). These results are consistent with the cytological data (Fig. 4B). Large tumor cells and many leukocytes were present in the ascites. After Vγ9Vδ2 T-cell injection, a large number of small mononuclear lymphocytes, presumably the Vγ9Vδ2 T cells themselves, were observed in ascites. The number of large tumor cells was gradually reduced by the repetitive injections of Vγ9Vδ2 T cells. In addition, many polymorphonuclear leukocytes were recruited into the ascites after zoledronate injection. The cytotoxic activity of Vγ9Vδ2 T cells was also examined in vitro (Fig. 4D). When Vγ9Vδ2 T cells from patient 2325 were cocultured with autologous $EpCAM^+$ tumor cells in vitro, Vγ9Vδ2 T cells attached and killed tumor cells (movie clip S1). These results indicated that Vγ9Vδ2 T cells indeed recognized tumor cells and exert antitumor activity.

Clinical outcome

Clinical outcomes are summarized in Table 3. Patients 2305 and 2336 were withdrawn from the study after a single round of injections, due to disease progression. Patients 2307 and 2334 were withdrawn after one and three doses of Vγ9Vδ2 T cells due to aspiration pneumonia and bacterial infection of the central venous catheter, respectively (although both patients experienced relief of their clinical symptoms and showed promising signs of immunological reactivity reflected by induction of IFN-γ and the reduction of tumor cells in ascites). As shown in Figure 4C, bloody ascites of patient 2325 became clear after the treatment. In addition, the massive retention of ascites was no longer present (Fig. 5A). Ascites was also reduced and almost disappeared in patient 2328 (Fig. 5B); therefore he received an additional two rounds of injections. Excellent palliation of symptoms was observed in these patients. However, the clinical benefits of i.p. Vγ9Vδ2 T-cell injection were restricted to the local control of malignant ascites. Patients 2325 and 2328 developed mediastinal lymph node metastasis and bone metastasis, respectively.

Adverse events

None of the patients experienced abdominal pain or any other toxicity related to i.p. injection of Vγ9Vδ2 T cells. The most commonly observed treatment-related adverse events were fever (Grade 2: $n = 3$) and zoledronate-induced hypocalcemia (Grade 3: $n = 4$) (Tables 3 and S1). These events were generally mild-to-moderate in intensity and reversible. In contrast, most adverse events and symptoms were due to end-stage gastric cancer with peritoneal dissemination and disease progression, namely, loss of protein (Grade 2: $n = 1$, and Grade 3: $n = 5$) and electrolyte disorders (Grade 3: $n = 3$, and Grade 4: $n = 2$). Peritoneal dissemination caused serious complications, including intestinal obstruction and massive ascites, associated with weight loss, bloating, constipation, nausea, insomnia, and abdominal pain. Aspiration pneumonia (Grade 3) and disseminated intravascular coagulation (Grade 2) was observed in patients 2305 and 2319, respectively. Central venous catheter infection was detected in patients 2325 and 2334 (Grade 2). None of these adverse events was directly related to the administration of Vγ9Vδ2 T cells and there were no treatment-related deaths.

Discussion

We report here the direct evidence that adoptively transferred Vγ9Vδ2 T cells do indeed recognize tumor cells and exert antitumor effector activity in vivo. Previously, we had conducted a clinical trial of adoptive Vγ9Vδ2 T-cell transfer therapy for non-small cell lung cancer in patients who were refractory to other treatments [12, 13]. Autologous Vγ9Vδ2 T-cells were expanded ex vivo using zoledronate and IL-2, and administered six times at 2-week intervals. The cultured cells were well-tolerated and some clinical benefit was observed in some patients in whom Vγ9Vδ2 T cells were able to survive and expand [12, 13]. However, it remained to be determined whether transferred Vγ9Vδ2 T cells infiltrated into the tumor and exerted antitumor effector functions in vivo. Therefore, we conducted a trial of adoptive Vγ9Vδ2 T-cell therapy for patients with malignant ascites caused by advanced

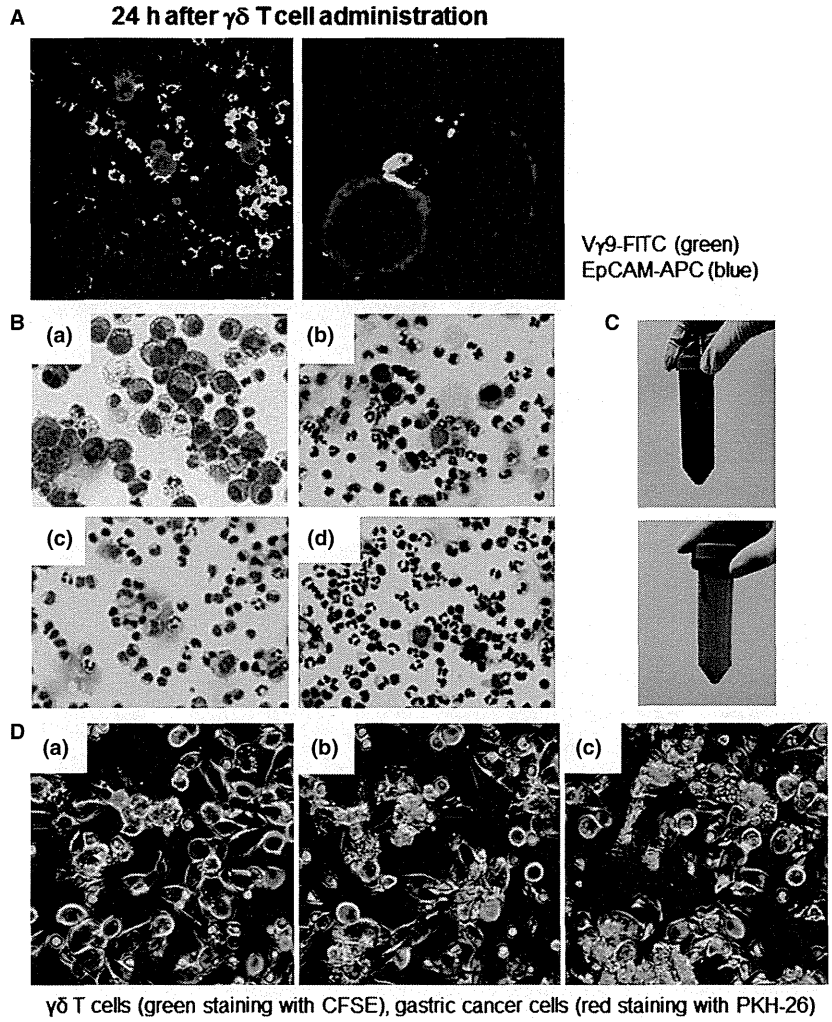

Figure 4. The cellular components and appearance of the ascites fluid. (A) The ascites fluid was harvested 24 h after Vγ9Vδ2 T-cell injection; the cells were stained with anti-TCRVγ9-FITC and anti-EpCAM-APC mAbs and examined by confocal fluorescence microscopy. The EpCAM$^+$ tumor cells (blue) are attached to and surrounded by Vγ9Vδ2 T cells (green) in ascites after Vγ9Vδ2 T-cell injections. Magnification was 150× on the left and 600× on the right. (B) Smears were prepared, air-dried, and stained with Diff-Quik (Sysmex, Kobe, Japan) according to the manufacturer's instructions. Cell morphology was evaluated using bright field microscopy (OLYMPUS BX41 with Canon EOS Kiss X4 digital camera, OLYMPUS, Tokyo, Japan, magnification 200×). Data from patient 2328 on day 0 (a: before zoledronate i.v.), day 9 (b: 24 h after 2nd Vγ9Vδ2 T-cell injection), day 21 (c: before zoledronate i.p.), and day 22 (d: 4 h after Vγ9Vδ2 T-cell injection) are shown. (C) The appearance of ascites from patient 2325 before and after four courses of Vγ9Vδ2 T-cell injections. (D) γδ T cells from patient 2325 (green staining with CFSE) recognized and killed autologous EpCAM$^+$ gastric cancer cells purified from ascites fluid (red staining with PKH-26), by direct contact. Tumor cells were attacked by the γδ T cells; collapse of the cell membranes led to apoptosis. It took approximately 2 h to progress from (a) to (c). Movie clip S1 is also provided.

gastric cancer. PBMC were harvested by apheresis; Vγ9Vδ2 T cells were similarly prepared with zoledronate and IL-2; Vγ9Vδ2 T cells were injected weekly into the peritoneal cavity, four times in total (Fig. 1B). Direct injection of Vγ9Vδ2 T cells into the peritoneal cavity allows them direct access to the tumor cells, bypassing the difficulties of recruitment of transferred Vγ9Vδ2 T-cells into solid tumors.

As shown in Figure 4A, many Vγ9Vδ2 T cells attached to each EpCAM$^+$ tumor cell in the ascites 24 h after their i.p. injection. Concomitantly, IFN-γ was detected in ascites with kinetics similar to the increased number of Vγ9Vδ2 T cells (Fig. 3B). The number of tumor cells in ascites was significantly reduced even after the first cell transfer and remained substantially lower during the course of the treatment (Fig. 3C). These results document tumor cell recognition and antitumor activity of Vγ9Vδ2 T cells in vivo. When autologous tumor cells were isolated by anti-EpCAM magnetic beads and cocultured with autologous zoledronate-expanded Vγ9Vδ2 T cells,

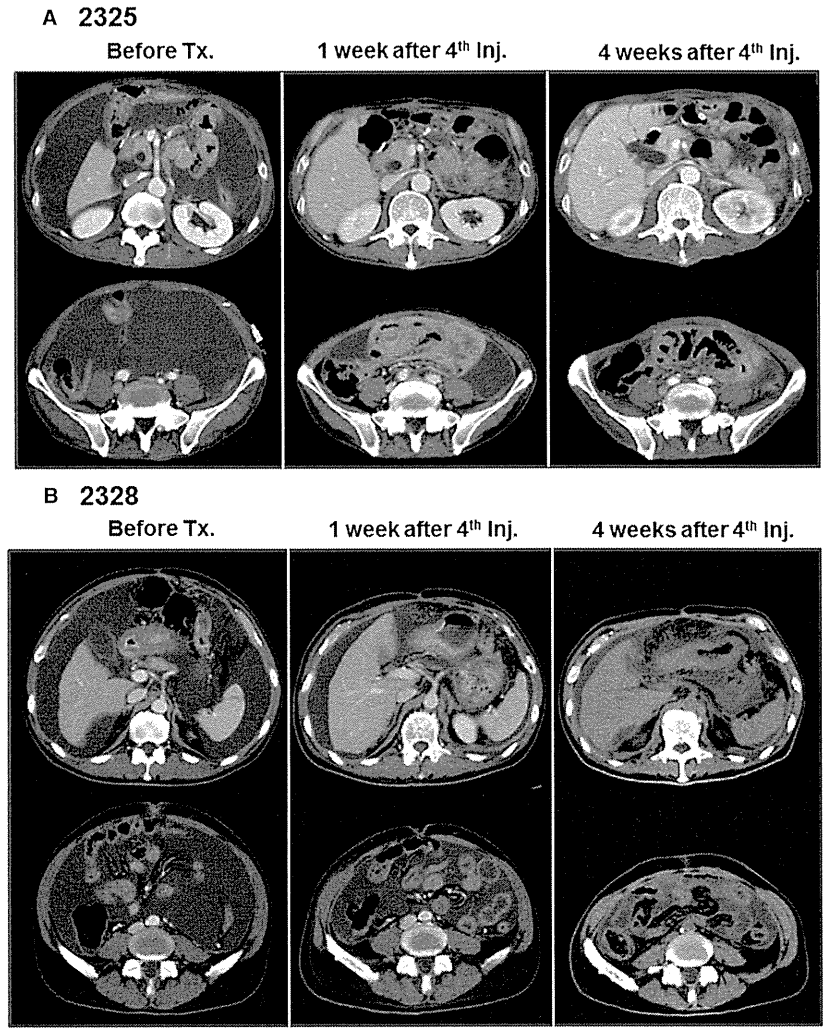

Figure 5. Computed tomography findings in patients 2325 (A) and 2328 (B). Retention of a large amount of ascites was observed before treatment (left panels). The amount of ascites was reduced 1 week (middle panels) and 4 weeks (right panels) after four courses of Vγ9Vδ2 T-cell injections.

Vγ9Vδ2 T cells indeed recognized and killed autologous tumor cells (Fig. 4D and movie clip S1). Such antitumor activity of i.p. Vγ9Vδ2 T cells resulted in some remarkable clinical effects. While the appearance of ascites was initially bloody in patient 2325, it became clear after i.p. Vγ9Vδ2 T-cell treatment (Fig. 4C). The reduction in ascites fluid was confirmed by computed tomography in patients 2325 and 2328 (Fig. 5). These results indicate that i.p. Vγ9Vδ2 T-cell injection combined with zoledronate contributed to the local control of malignant ascites in some patients with gastric cancer for whom no standard therapy apart from paracentesis was available.

NBPs such as zoledronate are widely used in the clinic for the treatment of bone metastases and are known as potent stimulators of Vγ9Vδ2 T cells [32]. Zoledronate blocks the mevalonate pathway, leading to intracellular accumulation of IPP, its isomer dimethylallyl pyrophosphate (DMAPP) and ApppI [24, 33, 34]. Because Vγ9Vδ2 T cells recognize these mevalonate metabolites in tumor cells, the high amounts of IPP and ApppI in zoledronate-treated tumor cells contributes to their recognition and lysis [35]. In the present study, zoledronate was administered 24 h prior to i.p. Vγ9Vδ2 T-cell injection with the aim of presensitizing the tumor cells. We injected zoledronate either i.v. or i.p. and compared these routes of injection (Fig. 1B). As shown in Figure 3B, smaller amounts of IFN-γ in ascites were detected in two of six patients after i.v. zoledronate injection, while higher amounts were found in ascites of all four patients who received i.p. zoledronate. These results are consistent with pharmacokinetic data for zoledronate, indicating that serum concentrations decline rapidly after infusion [31].

Table 3. Clinical outcome

Patient ID	Numbers of γδ T-cell injection	Adverse events (Grade, CTCAE v. 4.0)	Clinical outcome	
			Ascites	Others
2305	1	Rectal obstruction (3)[1]	No change	Growth of primary lesion
2307	1	Aspiration (3)[1], nausea (3),tumor pain (3), insomnia (2), hypoalbuminemia (2)	No change	Pleural effusion
2319	4	Fatigue (3), weight loss (3), hyponatremia (4), hypocalcemia (3), hypoalbuminemia (3), hypophosphatemia (3), female genital tract fistula (1), urinary tract infection (3), depressed level of consciousness (3), disseminated intravascular coagulation (2), lymphocyte count decreased (3)	No change	Obstructive jaundice due to the growth of primary lesion
2325	4	Fever (2), bloating (2), constipation (2), nausea (2), anemia (1), hypoalbuminemia (3), hypophosphatemia (3), hypocalcemia (3), urinary tract infection (2), insomnia (2), tumor pain (3), central venous catheter-related infection (2)	Disappeared	Mediastinal lymphadenopathy, pleural effusion, carcinomatous lymphangiosis
2334	3	Fever (2), nausea (2), insomnia (2), central venous catheter-related infection (2)[1], tumor pain (3), anemia (3), hypocalcemia (3), hypoalbuminemia (3), palmar-plantar erythrodysesthesia syndrome (1)	No change	Metastasis to ovary
2336	1	Tumor pain (3), hypoalbuminemia (3), hypocalcemia (3), hyponatremia (3), hyperkalemia (4)	No change	Poor performance status[1], metastasis to bladder, ovary and skin
2328	4 (+2)	Fever (2), gastritis (2), constipation (2), hypoalbuminemia (3), lymphocyte count decreased (3)	Reduced	Bone metastasis

[1]Cause for discontinuance.

When we harvest ascites 2–8 h after i.p. zoledronate injection, ascites fluid contained the sufficient amount of zoledronate to expand Vγ9Vδ2 T cell, suggesting they might inhibit farnesyl pyrophosphate (FPP) synthase activity in the tumor cells at this time point (Fig. S1). However, Vγ9Vδ2 T cell did not respond to the ascites fluid harvested after i.v. zoledronate injection. Therefore, the zoledronate concentration in the ascites might not be sufficient for the inhibition of FPP synthase activity after i.v. administration. While the optimum dose and timing of zoledronate administration remain to be elucidated, the local administration of zoledronate is desired to inhibit FPP synthase and sensitize tumor cells in the abdominal cavity to efficient Vγ9Vδ2 T-cells recognition.

In addition to the direct cytotoxic activity of Vγ9Vδ2 T-cells on the tumor cells, their activation results in release of many cytokines and chemokines that may lead to the recruitment and activation of other immune cells. It has been reported that Vγ9Vδ2 T cells induce dendritic cell maturation [36], B-cell activation [37], and polarization of Th1 immune responses [38]. We observed marked recruitment of neutrophils into the peritoneal cavity in this study (Fig. 4B); zoledronate alone induced granulocyte recruitment, suggesting that NBPs induce γδ T cell-independent neutrophil recruitment in humans. Recently, Norton et al. [39] reported that intraperitoneal injection of alendronate, one of the FDA-approved NBPs, induced peritoneal inflammation in mice. In their model, neutrophil recruitment depended on mast cells and IL-1R signaling. As mice lack the counterpart of human Vγ9Vδ2 T cells and thus cannot respond to IPP and NBPs, the mechanism of peritoneal inflammation in mice might be different from our human study. Consistent with a previous reports that Vγ9Vδ2 T-cell activation-induced neutrophil migration and increased their phagocytic potential and release of α-defensins [40], and that γδ T cells rapidly induce CXCL8-mediated migration of neutrophils [41], infiltration of neutrophils was sustained after i.p. Vγ9Vδ2 T-cell injection in this study (Fig. 4B). Despite the recruitment of many neutrophils into the peritoneal cavity, patients did not complain of abdominal pain and did not display any signs of peritonitis except retention of ascites after Vγ9Vδ2 T-cell injection.

The combination of i.p. Vγ9Vδ2 T-cell injection and zoledronate for the treatment of malignant ascites had acceptable tolerability without unexpected severe or long-lasting adverse events. Because patients with severe peritoneal dissemination and malignant ascites are generally in a poor condition, adverse events were frequent; many of them were not associated with cell transfer (Tables 3 and S1). However, pyrexia was probably associated with the release of proinflammatory cytokines induced by zoledronate and Vγ9Vδ2 T-cell injection. The local i.p. injection of zoledronate and Vγ9Vδ2 T cells might reduce the

systemic adverse events associated with the release of pro-inflammatory cytokines. Though the kinetics of IL-1β, IL-8, and TNF-α production in ascites fluid were similar with that of IFN-γ, the changes of these cytokines were not detected in the patients' serum (data not shown). The IL-6 was elevated before the treatment in many of these advanced cancer patients, the changes associated with zoledronate and/or Vγ9Vδ2 T-cells were not clear. The alterations in laboratory parameters were rarely considered clinically relevant to the treatment except for hypocalcemia caused by zoledronate.

The patients in this study received S-1 plus cisplatin, S-1 plus docetaxel, or docetaxel alone as a standard regimen for the treatment of unresectable or recurrent gastric cancer prior to the Vγ9Vδ2 T-cell therapy (Table 1) [17, 18]. It has been reported that the overall median survival time in treatment-naïve patients with malignant ascites was approximately 5 months irrespective of the regimen received [16, 42, 43]. Once patients have become refractory to these chemotherapies, it is unlikely that they will experience a survival benefit from any treatment. In such cases, paracentesis and diuretics are primarily used in managing malignant ascites, neither of which is an anti-cancer treatment but solely palliative [15]. In contrast, the i.p. injection of Vγ9Vδ2 T cells combined with zoledronate directly affects the tumor cells and reduces their number in the peritoneal cavity, as well as decreasing the amount of ascites fluid, leading to palliation of the symptoms of malignant ascites.

Although the i.p. Vγ9Vδ2 T-cell injection and zoledronate treatment is unlikely to impact overall survival in such advanced disease, especially with metastasis, our results show a clear clinical benefit for the local control of malignant ascites (Fig. 5). We are planning to conduct a new clinical trial for treatment-naïve patients with peritoneal dissemination to evaluate the survival benefit of this treatment. Furthermore, combinations of this newly emerging therapy with established surgical, radiotherapy, and chemotherapy treatments are expected to improve the survival of cancer patients in future.

Acknowledgements

This study was supported in part by a Grant-in-Aid for Scientific Research of the Ministry of Education, Culture, Sports, Science and Technology (K. K.). We thank Makoto Kondo, Takamichi Izumi, and Takuya Takahashi for performing the γδ T cell cultures; Nao Fujieda, Atsushi Kondo, Kaori Kanbara, and Ryuji Maekawa for immunological monitoring and laboratory assistance; Takashige Kondo, Yoko Yamashita, Tomoko Ishida, Haruka Matsushita, Yuki Nagasawa, Hiroki Yoshihara, and Akiko Fukuzawa for administrative supports.

Conflict of Interest

Dr. Kazuhiro Kakimi received research support from Medinet Co. Ltd. (Yokohama, Japan). The costs of the entire γδ T cell culture production and part of the immunological assays were covered by Medinet Co. Ltd. The study sponsors had no involvement in study design; collection, analysis, and interpretation of data; writing the report; and the decision to submit the report for publication. All other authors have declared there are no financial conflicts of interest related to this work.

References

1. Hayday, A. C. 2000. γδ cells: a right time and a right place for a conserved third way of protection. Annu. Rev. Immunol. 18:975–1026.
2. Carding, S. R., and P. J. Egan. 2002. γδ T cells: functional plasticity and heterogeneity. Nat. Rev. Immunol. 2:336–345.
3. Triebel, F., and T. Hercend. 1989. Subpopulations of human peripheral T γδ lymphocytes. Immunol. Today 10:186–188.
4. Bonneville, M., and E. Scotet. 2006. Human Vgamma9Vdelta2 T cells: promising new leads for immunotherapy of infections and tumors. Curr. Opin. Immunol. 18:539–546.
5. Riganti, C., M. Massaia, M. S. Davey, and M. Eberl. 2012. Human gammadelta T-cell responses in infection and immunotherapy: common mechanisms, common mediators? Eur. J. Immunol. 42:1668–1676.
6. Wilhelm, M., V. Kunzmann, S. Eckstein, P. Reimer, F. Weissinger, T. Ruediger, et al. 2003. γδ T cells for immune therapy of patients with lymphoid malignancies. Blood 102:200–206.
7. Dieli, F., D. Vermijlen, F. Fulfaro, N. Caccamo, S. Meraviglia, G. Cicero, et al. 2007. Targeting human γδ T cells with zoledronate and interleukin-2 for immunotherapy of hormone-refractory prostate cancer. Cancer Res. 67:7450–7457.
8. Bennouna, J., E. Bompas, E. M. Neidhardt, F. Rolland, I. Philip, C. Galea, et al. 2008. Phase-I study of Innacell gammadelta, an autologous cell-therapy product highly enriched in gamma9delta2 T lymphocytes, in combination with IL-2, in patients with metastatic renal cell carcinoma. Cancer Immunol. Immunother. 57:1599–1609.
9. Kobayashi, H., Y. Tanaka, J. Yagi, N. Minato, and K. Tanabe. 2011. Phase I/II study of adoptive transfer of gammadelta T cells in combination with zoledronic acid and IL-2 to patients with advanced renal cell carcinoma. Cancer Immunol. Immunother. 60:1075–1084.
10. Kondo, M., K. Sakuta, A. Noguchi, N. Ariyoshi, K. Sato, S. Sato, et al. 2008. Zoledronate facilitates large-scale ex vivo expansion of functional gammadelta T cells from

cancer patients for use in adoptive immunotherapy. Cytotherapy 10:842–856.
11. Sato, K., M. Kondo, K. Sakuta, A. Hosoi, S. Noji, M. Sugiura, et al. 2009. Impact of culture medium on the expansion of T cells for immunotherapy. Cytotherapy 11:936–946.
12. Nakajima, J., T. Murakawa, T. Fukami, S. Goto, T. Kaneko, Y. Yoshida, et al. 2010. A phase I study of adoptive immunotherapy for recurrent non-small-cell lung cancer patients with autologous γδ T cells. Eur. J. Cardiothorac. Surg. 37:1191–1197.
13. Sakamoto, M., J. Nakajima, T. Murakawa, T. Fukami, Y. Yoshida, T. Murayama, et al. 2011. Adoptive immunotherapy for advanced non-small cell lung cancer using zoledronate-expanded gammadeltaTcells: a phase I clinical study. J. Immunother. 34:202–211.
14. Dupont, J. B., Jr., J. R. Lee, G. R. Burton, and I. Cohn Jr.. 1978. Adenocarcinoma of the stomach: review of 1,497 cases. Cancer 41:941–947.
15. Cavazzoni, E., W. Bugiantella, L. Graziosi, M. Franceschini, and A. Donini. 2013. Malignant ascites: pathophysiology and treatment. Int. J. Clin. Oncol. 18:1–9.
16. Imamoto, H., K. Oba, J. Sakamoto, H. Iishi, H. Narahara, T. Yumiba, et al. 2011. Assessing clinical benefit response in the treatment of gastric malignant ascites with non-measurable lesions: a multicenter phase II trial of paclitaxel for malignant ascites secondary to advanced/recurrent gastric cancer. Gastric Cancer 14:81–90.
17. Koizumi, W., H. Narahara, T. Hara, A. Takagane, T. Akiya, M. Takagi, et al. 2008. S-1 plus cisplatin versus S-1 alone for first-line treatment of advanced gastric cancer (SPIRITS trial): a phase III trial. Lancet Oncol. 9:215–221.
18. Lenz, H. J., F. C. Lee, D. G. Haller, D. Singh, A. B. Benson III, D. Strumberg, et al. 2007. Extended safety and efficacy data on S-1 plus cisplatin in patients with untreated, advanced gastric carcinoma in a multicenter phase II study. Cancer 109:33–40.
19. Ishigami, H., J. Kitayama, S. Kaisaki, A. Hidemura, M. Kato, K. Otani, et al. 2010. Phase II study of weekly intravenous and intraperitoneal paclitaxel combined with S-1 for advanced gastric cancer with peritoneal metastasis. Ann. Oncol. 21:67–70.
20. Heiss, M. M., P. Murawa, P. Koralewski, E. Kutarska, O. O. Kolesnik, V. V. Ivanchenko, et al. 2010. The trifunctional antibody catumaxomab for the treatment of malignant ascites due to epithelial cancer: results of a prospective randomized phase II/III trial. Int. J. Cancer 127:2209–2221.
21. Glimelius, B., K. Hoffman, U. Haglund, O. Nyren, and P. O. Sjoden. 1994. Initial or delayed chemotherapy with best supportive care in advanced gastric cancer. Ann. Oncol. 5:189–190.
22. Pyrhonen, S., T. Kuitunen, P. Nyandoto, and M. Kouri. 1995. Randomised comparison of fluorouracil, epidoxorubicin and methotrexate (FEMTX) plus supportive care with supportive care alone in patients with non-resectable gastric cancer. Br. J. Cancer 71:587–591.
23. Kang, J. H., S. I. Lee, D. H. Lim, K.-W. Park, S. Y. Oh, H.-C. Kwon, et al. 2012. Salvage chemotherapy for pretreated gastric cancer: a randomized phase III trial comparing chemotherapy plus best supportive care with best supportive care alone. J. Clin. Oncol. 30:1513–1518.
24. Gober, H. J., M. Kistowska, L. Angman, P. Jeno, L. Mori, and G. De Libero. 2003. Human T cell receptor gammadelta cells recognize endogenous mevalonate metabolites in tumor cells. J. Exp. Med. 197:163–168.
25. Clézardin, P. 2011. Bisphosphonates' antitumor activity: an unravelled side of a multifaceted drug class. Bone 48:71–79.
26. Japanese Gastric Cancer Association. 2011. Japanese classification of gastric carcinoma: 3rd English edition. Gastric Cancer 14:101–112.
27. Kondo, M., T. Izumi, N. Fujieda, A. Kondo, T. Morishita, H. Matsushita, et al. 2011. Expansion of human peripheral blood gammadelta T cells using zoledronate. J. Vis. Exp. e3182, doi: 10.3791/3182.
28. Izumi, T., M. Kondo, T. Takahashi, N. Fujieda, A. Kondo, N. Tamura, et al. 2013. Ex vivo characterization of gammadelta T-cell repertoire in patients after adoptive transfer of Vgamma9Vdelta2 T cells expressing the interleukin-2 receptor beta-chain and the common gamma-chain. Cytotherapy 15:481–491.
29. Fischer, K., R. Andreesen, and A. Mackensen. 2002. An improved flow cytometric assay for the determination of cytotoxic T lymphocyte activity. J. Immunol. Methods 259:159–169.
30. Idrees, A. S. M., T. Sugie, C. Inoue, K. Murata-Hirai, H. Okamura, C. T. Morita, et al. 2013. Comparison of γδ T cell responses and farnesyl diphosphate synthase inhibition in tumor cells pretreated with zoledronic acid. Cancer Sci. 104:536–542.
31. Chen, T., J. Berenson, R. Vescio, R. Swift, A. Gilchick, S. Goodin, et al. 2002. Pharmacokinetics and pharmacodynamics of zoledronic acid in cancer patients with bone metastases. J. Clin. Pharmacol. 42:1228–1236.
32. Kunzmann, V., E. Bauer, J. Feurle, F. Weissinger, H. P. Tony, and M. Wilhelm. 2000. Stimulation of gammadelta T cells by aminobisphosphonates and induction of antiplasma cell activity in multiple myeloma. Blood 96:384–392.
33. Roelofs, A. J., M. Jauhiainen, H. Monkkonen, M. J. Rogers, J. Monkkonen, and K. Thompson. 2009. Peripheral blood monocytes are responsible for gammadelta T cell activation induced by zoledronic acid through accumulation of IPP/DMAPP. Br. J. Haematol. 144:245–250.
34. Monkkonen, H., S. Auriola, P. Lehenkari, M. Kellinsalmi, I. E. Hassinen, J. Vepsalainen, et al. 2006. A new

endogenous ATP analog (ApppI) inhibits the mitochondrial adenine nucleotide translocase (ANT) and is responsible for the apoptosis induced by nitrogen-containing bisphosphonates. Br. J. Pharmacol. 147:437–445.
35. Benzaid, I., H. Monkkonen, V. Stresing, E. Bonnelye, J. Green, J. Monkkonen, et al. 2011. High phosphoantigen levels in bisphosphonate-treated human breast tumors promote Vgamma9Vdelta2 T-cell chemotaxis and cytotoxicity in vivo. Cancer Res. 71:4562–4572.
36. Ismaili, J., V. Olislagers, R. Poupot, J. J. Fournie, and M. Goldman. 2002. Human gamma delta T cells induce dendritic cell maturation. Clin. Immunol. 103:296–302.
37. Brandes, M., K. Willimann, A. B. Lang, K. H. Nam, C. Jin, M. B. Brenner, et al. 2003. Flexible migration program regulates gamma delta T-cell involvement in humoral immunity. Blood 102:3693–3701.
38. Poccia, F., M. L. Gougeon, C. Agrati, C. Montesano, F. Martini, C. D. Pauza, et al. 2002. Innate T-cell immunity in HIV infection: the role of Vgamma9Vdelta2 T lymphocytes. Curr. Mol. Med. 2:769–781.
39. Norton, J. T., T. Hayashi, B. Crain, J. S. Cho, L. S. Miller, M. Corr, et al. 2012. Cutting edge: nitrogen bisphosphonate-induced inflammation is dependent upon mast cells and IL-1. J. Immunol. 188:2977–2980.
40. Agrati, C., E. Cimini, A. Sacchi, V. Bordoni, C. Gioia, R. Casetti, et al. 2009. Activated Vγ9Vδ2 T cells trigger granulocyte functions via MCP-2 release. J. Immunol. 182:522–529.
41. Caccamo, N., C. La Mendola, V. Orlando, S. Meraviglia, M. Todaro, G. Stassi, et al. 2011. Differentiation, phenotype, and function of interleukin-17-producing human Vγ9Vδ2 T cells. Blood 118:129–138.
42. Yamao, T., Y. Shimada, K. Shirao, A. Ohtsu, N. Ikeda, I. Hyodo, et al. 2004. Phase II study of sequential methotrexate and 5-fluorouracil chemotherapy against peritoneally disseminated gastric cancer with malignant ascites: a report from the Gastrointestinal Oncology Study Group of the Japan Clinical Oncology Group, JCOG 9603 Trial. Jpn. J. Clin. Oncol. 34:316–322.
43. Oh, S. Y., H. C. Kwon, S. Lee, D. M. Lee, H. S. Yoo, S. H. Kim, et al. 2007. A phase II study of oxaliplatin with low-dose leucovorin and bolus and continuous infusion 5-fluorouracil (modified FOLFOX-4) for gastric cancer patients with malignant ascites. Jpn. J. Clin. Oncol. 37:930–935.

Supporting Information

Additional Supporting Information may be found in the online version of this article:

Figure S1. The concentration of zoledronate was estimated by the Vγ9Vδ2 T-cell bioassay. PBMCs from healthy donor were stimulated with indicated amount of zoledronate in AlyS203 medium containing 1000 IU/mL human recombinant IL-2 and 10% pooled human serum. After 14 day-culture, expansion of Vγ9Vδ2 T cell was measured by flow cytometry to prepare the standard curve. Same donor-derived PBMCs were cultured in IL-2 containing medium and in the presence of 10% patient ascites fluid for 14 days. The concentration of zoledronate was estimated by the expansion of Vγ9Vδ2 T cell using the standard curve.
Movie clip S1. Patient's Vγ9Vδ2 T cells recognize and kill autologous tumor cells.
Table S1. Adverse events.
Table S2. % Cytotoxicity of Vγ9Vδ2 T cells against Daudi cells w/o zoledronate treatment.

Ann Surg Oncol (2014) 21:2105–2112
DOI 10.1245/s10434-014-3503-2

Annals of
SURGICAL ONCOLOGY
OFFICIAL JOURNAL OF THE SOCIETY OF SURGICAL ONCOLOGY

ORIGINAL ARTICLE – UROLOGIC ONCOLOGY

Prognostic Significance of CD204-Positive Macrophages in Upper Urinary Tract Cancer

Takashi Ichimura, MD[1], Teppei Morikawa, MD, PhD[1], Taketo Kawai, MD, PhD[2], Tohru Nakagawa, MD, PhD[2], Hirokazu Matsushita, MD, PhD[3], Kazuhiro Kakimi, MD, PhD[3], Haruki Kume, MD, PhD[2], Shumpei Ishikawa, MD, PhD[4], Yukio Homma, MD, PhD[2], and Masashi Fukayama, MD, PhD[1]

[1]Department of Pathology, Graduate School of Medicine, The University of Tokyo, Tokyo, Japan; [2]Department of Urology, Graduate School of Medicine, The University of Tokyo, Tokyo, Japan; [3]Department of Immunotherapeutics (Medinet), The University of Tokyo Hospital, Tokyo, Japan; [4]Department of Genomic Pathology, Medical Research Institute, Tokyo Medical and Dental University, Tokyo, Japan

ABSTRACT

Background. Evidence suggests that CD204-positive ($CD204^+$) tumor-infiltrating macrophages are associated with aggressive behavior of various cancers; however, the clinical, pathological, and prognostic associations of tumor-infiltrating $CD204^+$ macrophages in urothelial cancer have not been reported.

Methods. A tissue microarray was constructed from the centers and peripheries of 171 upper urinary tract cancers treated with nephroureterectomy. CD204 immunohistochemistry was performed. The density of $CD204^+$ cells was calculated using image analysis software, and survival analyses were performed using the Kaplan–Meier method and multivariate Cox proportional hazards regression models.

Results. High $CD204^+$ cell density at the centers and peripheries of tumors was significantly associated with several adverse prognostic factors, including sessile architecture, histological high-grade, presence of lymphovascular invasion, concomitant carcinoma in situ, higher tumor stage, and lymph node metastasis. High $CD204^+$ cell density was significantly associated with shorter metastasis-free and cancer-specific survival (log-rank $p < 0.001$) and shorter metastasis-free survival in multivariate analysis.

Conclusions. A high density of tumor-infiltrating $CD204^+$ macrophages was associated with aggressive behavior of upper urinary tract cancer. Our results suggest that a specific immune microenvironment may be associated with the biological behavior of urothelial cancer and that CD204 may serve as a novel prognostic biomarker for these tumors.

Tumor tissue comprises variable numbers of cancer and stromal cells, and the tumor microenvironment plays important roles in the biological behavior of cancer.[1–6] Macrophages, which contribute to the host's immune response, are the most abundant stromal cells in tumors.[7] Macrophages possess tumor suppressive (M1) and tumor-supportive (M2) functions.[8] M2-polarized macrophages express high levels of CD204 (also called scavenger receptor A).[9] Recent studies show that a high number of tumor-infiltrating CD204-positive ($CD204^+$) macrophages is associated with worse patient outcome in a variety of cancers.[10–16] However, the role of $CD204^+$ macrophages in urothelial cancer has not been reported. We therefore examined the clinicopathological and prognostic associations of tumor-infiltrating $CD204^+$ macrophages in patients with upper urinary tract cancer.

MATERIALS AND METHODS

Study Population

A total of 171 patients with upper urinary tract cancer who underwent nephroureterectomy at The University of Tokyo Hospital from 1996 to 2012 were included in this study. No

Electronic supplementary material The online version of this article (doi:10.1245/s10434-014-3503-2) contains supplementary material, which is available to authorized users.

First Received: 24 July 2013;
Published Online: 4 February 2014

M. Fukayama, MD, PhD
e-mail: mfukayama-tky@umin.org

patient received neoadjuvant chemotherapy. In 31 cases, bladder cancer was found and treated before or at the time of nephroureterectomy. All research protocols in the present study were approved by our Institutional Review Board.

Histopathological Evaluation

Hematoxylin and eosin (H&E)-stained slides of all cases were reviewed by a pathologist (TM) without knowledge of clinical outcomes. Tumor histology and grade were defined according to the World Health Organization/International Society of Urologic Pathology consensus classification.[17] All tumors (103 pelvic cancers and 68 ureteral cancers) were histologically diagnosed as urothelial carcinomas. Tumors were staged according to the TNM classification system.[18] Lymphovascular invasion was examined using H&E and Elastica van Gieson staining.

Tissue Microarray Construction

H&E-stained slides were evaluated for the presence of the tumor center and the periphery. The tumor periphery was defined as the area of invasive margin or as the area where cancer cells were closest to the lamina propria for non-invasive tumors. For each tumor specimen, H&E-stained slides containing the tumor center and the periphery were selected. Using a tissue microarrayer (Beecher Instruments Inc., Sun Prairie, WI, USA), each region in the donor paraffin block was cored with a needle 2 mm in diameter and transferred to the recipient paraffin block.[19]

Immunohistochemical Analysis

Preparation of sections from paraffin blocks was performed as previously described.[20] Immunohistochemical analysis of CD204 was performed using a mouse monoclonal antibody against human CD204 (clone SRA-E5, 1:500; Transgenic, Kumamoto, Japan) according to standard techniques for a Ventana Benchmark® XT Autostainer (Ventana Medical Systems, Tucson, AZ, USA). Antigen retrieval was carried out using Cell Conditioning Solution (CC1-Tris-based EDTA buffer, pH 8.0; Ventana Medical Systems). Visualization was achieved using the I-VIEW DAB Universal Kit (Ventana Medical Systems) and hematoxylin counterstaining.

Image Analysis

Images of immunostained slides were digitized at 20× magnification using the NanoZoomer Digital Pathology (NDP) System (Hamamatsu Photonics, Hamamatsu, Japan). For digital quantification, image analysis software (Tissue Studio v.3.5; Definiens AG, Munich, Germany) was used to distinguish the $CD204^+$ macrophages.[21] The percentage of the area containing $CD204^+$ cells (summed area with $CD204^+$ cells/total measured area × 100) was calculated for each tissue microarray core.[14]

Statistical Analysis

All statistical analyses were performed using SAS software (Version 9.3, SAS Institute, Cary, NC, USA). All p values were two-sided. Differences were considered significant at $p < 0.05$. For categorical data, the Chi square test was performed. The Kaplan–Meier method and log-rank test were used to analyze survival. To control for confounding variables, multivariate Cox proportional hazards regression models were used. The multivariate models initially included gender, age at diagnosis, tumor side, tumor location, tumor architecture, tumor grade, lymphovascular invasion, concomitant carcinoma in situ, tumor stage, lymph node metastasis, and adjuvant chemotherapy. Tumor stage was dichotomized (pTa–pT1 vs. pT2–pT4) to be consistent with previous studies.[22–26] A backward elimination was performed using a threshold of $p = 0.05$; however, CD204 status, tumor stage, and lymph node metastasis were forced into the final models.

RESULTS

Distribution of Tumor-Infiltrating $CD204^+$ Macrophages in Upper Urinary Tract Cancer

Representative photomicrographs of CD204 immunohistochemistry are presented in Fig. 1. The median tumor-infiltrating $CD204^+$ cell density was 0.64 % (range 0.03–9.29 %) at the tumor center, and 0.81 % (range 0.03–12.43 %) at the tumor periphery. $CD204^+$ cell density of the two areas correlated positively (Spearman $r = 0.76$; $p < 0.0001$), and there was no significant difference between the tumor center and the periphery ($p > 0.05$, Wilcoxon signed-rank test). We divided the cases into high and low $CD204^+$ groups according to the median value of $CD204^+$ cell density.[14] High $CD204^+$ density at both the tumor center and the periphery was significantly associated with sessile architecture, histological high-grade, presence of lymphovascular invasion, concomitant carcinoma in situ, higher tumor stage, and lymph node metastasis (Table 1).

$CD204^+$ Macrophages and Clinical Outcome of Upper Urinary Tract Cancer

Patients with previous or concurrent bladder cancer ($n = 31$) were excluded from the survival analyses because

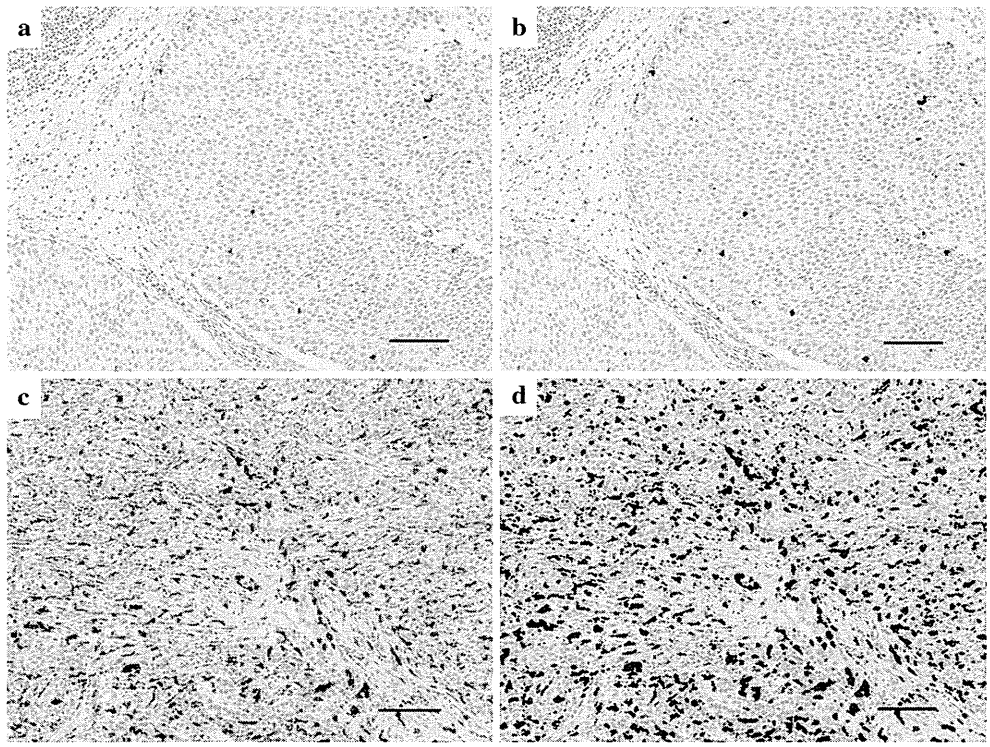

FIG. 1 Quantitation of $CD204^+$ macrophage density in upper urinary tract urothelial carcinoma. CD204 immunohistochemistry shows low (**a**) and high (**c**) infiltration of $CD204^+$ macrophages. Using image analysis software, immunopositive areas are highlighted in red, and the percentage of immunopositive area (summed area with $CD204^+$ macrophages/total measured area × 100) was calculated (**b**, **d**). *Bars* indicate 100 μm. *$CD204^+$* CD204-positive

they may affect the outcome of upper urinary tract cancer.[27] Among the 140 patients without bladder cancer at the time of nephroureterectomy, there were 58 bladder recurrences, 32 metastases, and 23 cancer-specific deaths during a median 56-month follow-up (interquartile range 25–86 months).

Kaplan–Meier analysis revealed that high $CD204^+$ density at both the tumor center and the periphery was significantly associated with shorter metastasis-free and cancer-specific survival (log-rank $p < 0.001$; Fig. 2). High $CD204^+$ density at both the tumor center and the periphery was also significantly associated with shorter metastasis-free survival in univariate and multivariate Cox models (Table 2). High $CD204^+$ density was significantly associated with shorter cancer-specific survival in univariate analysis, but the statistical significance was not achieved in multivariate analysis (Table 3). Lymphovascular invasion and lymph node metastasis were also significantly associated with shorter metastasis-free and cancer-specific survival in univariate and multivariate analyses. Tumor stage was not significantly associated with shorter metastasis-free and cancer-specific survival in multivariate analysis, consistent with previous studies.[24–26,28] $CD204^+$ density was not significantly associated with bladder recurrence-free survival in Kaplan–Meier analysis (Fig. 2) or in univariate and multivariate Cox models (Supplementary Table 1).

DISCUSSION

To our knowledge, the present study is the first to assess the clinicopathological and prognostic associations of $CD204^+$ macrophages in upper urinary tract cancer. We found that a high density of tumor-infiltrating $CD204^+$ cells was significantly associated with sessile architecture, histological high-grade, lymphovascular invasion, concomitant carcinoma in situ, higher tumor stage, and lymph node metastasis, which are adverse prognostic factors in upper urinary tract cancer.[29,30] Moreover, high $CD204^+$ cell density was significantly associated with shorter metastasis-free and cancer-specific survival. Our findings suggest that tumor-infiltrating $CD204^+$ macrophages are associated with aggressive behavior of upper urinary tract cancer.

A high density of tumor-infiltrating $CD204^+$ macrophages is associated with a poorer prognosis in lung,[10,12,13] pancreatic,[11,14,15] and esophageal carcinomas.[16] In two of these studies, the independent prognostic significance of CD204 expression was also shown using multivariate analysis.[12,14] In contrast, there was no prognostic

TABLE 1 Correlation between tumor-infiltrating CD204-positive macrophage density and clinicopathological features in patients with upper urinary tract cancer who underwent nephroureterectomy

Clinical or pathologic feature	Total *N*	CD204 (tumor center) [*n* (%)]		*p* value	CD204 (tumor periphery) [*n* (%)]		*p* value
		Low	High		Low	High	
All cases	171	85 (50)	86 (50)		85 (50)	86 (50)	
Gender				0.34			0.96
Men	119	62 (52)	57 (48)		59 (50)	60 (50)	
Women	52	23 (44)	29 (56)		26 (50)	26 (50)	
Age (years)				0.14			0.59
<70	93	51 (55)	42 (45)		48 (52)	45 (48)	
≥70	78	34 (44)	44 (56)		37 (47)	41 (53)	
Side				0.25			0.82
Left	86	39 (45)	47 (55)		42 (49)	44 (51)	
Right	85	46 (54)	39 (46)		43 (51)	42 (49)	
History of bladder cancer				0.81			0.81
No	140	69 (49)	71 (51)		69 (49)	71 (51)	
Yes	31	16 (52)	15 (48)		16 (52)	15 (48)	
Tumor location				0.03			0.23
Renal pelvis	103	58 (56)	45 (44)		55 (53)	48 (47)	
Ureter	68	27 (40)	41 (60)		30 (44)	38 (56)	
Tumor architecture				0.0037			0.0037
Papillary	126	71 (56)	55 (44)		71 (56)	55 (44)	
Sessile	45	14 (31)	31 (69)		14 (31)	31 (69)	
Grade				<0.0001			<0.0001
Low	19	18 (95)	1 (5.3)		19 (100)	0	
High	152	67 (44)	85 (56 %)		66 (43)	86 (57)	
Lymphovascular invasion				<0.0001			<0.0001
Absent	97	61 (63)	36 (37 %)		62 (64)	35 (36)	
Present	74	24 (32)	50 (68)		23 (31)	51 (69)	
Concomitant carcinoma in situ				0.0046			0.0002
Absent	88	53 (60)	35 (40)		56 (64)	32 (36)	
Present	83	32 (39)	51 (61)		29 (35)	54 (65)	
Tumor stage				<0.0001			<0.0001
pTa	37	34 (92)	3 (8.1)		35 (95)	2 (5.4)	
pTis	7	4 (57)	3 (43)		3 (43)	4 (57)	
pT1	31	17 (55)	14 (45)		21 (68)	10 (32)	
pT2	18	8 (44)	10 (56)		6 (33)	12 (67)	
pT3	69	22 (32)	47 (68)		19 (28)	50 (72)	
pT4	9	0	9 (100)		1 (11)	8 (89)	
Lymph node metastasis				0.0017			0.0081
Absent	152	82 (54)	70 (46)		81 (53)	71 (47)	
Present	19	3 (16)	16 (84)		4 (21)	15 (79)	

significance of $CD204^+$ macrophages in renal cell carcinoma[31] or lymphoma.[32] In the present study, univariate and multivariate analysis show that tumor-infiltrating $CD204^+$ cell density associated significantly with shorter metastatic-free survival. Statistical significance was not achieved for cancer-specific survival in multivariate analysis, probably owing to fewer events and lower statistical power. Our results suggest that tumor-infiltrating $CD204^+$ cell density may be a novel prognostic biomarker to predict metastasis in patients with upper urinary tract cancer.

To assess heterogeneity within a tumor, we evaluated two tissue cores taken from either the tumor center or the periphery for each case. While most previous studies on CD204 visually evaluated a few high-power

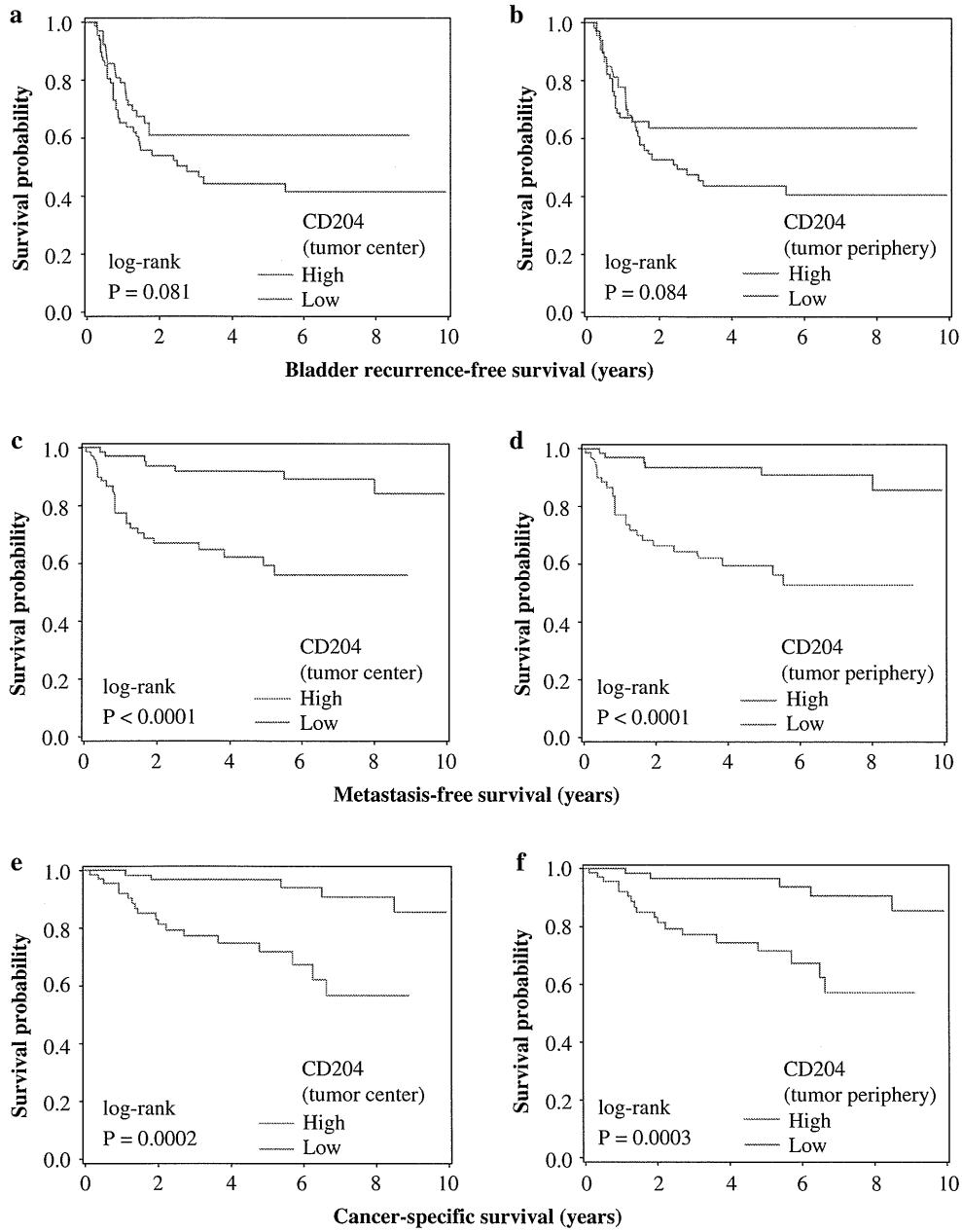

FIG. 2 Kaplan–Meier analysis of bladder recurrence-free survival (**a**, **b**), metastasis-free survival (**c** and **d**), and cancer-specific survival (**e**, **f**) after nephroureterectomy according to $CD204^+$ macrophage density at the tumor center (**a**, **e**) and periphery (**b**, **f**). *$CD204^+$* $CD204^+$-positive

fields,[10–13,16,32,33] here we evaluated $CD204^+$ cell density in a larger area (>6 mm^2 for each case) using validated image analysis software.[21] We found that $CD204^+$ cell density at the tumor center and the periphery strongly correlated, and that the associations of CD204 expression with clinicopathological features and patient outcomes were quite similar between them. Although further studies using whole slide sections are required to validate our findings,[34,35] our results suggest that $CD204^+$ cell density at either the tumor center or periphery may serve as a useful prognostic marker for upper urinary tract cancer.

Accumulating evidence suggests that tumor cells induce tumor-promoting $CD204^+$ macrophages to generate a specific microenvironment that supports tumor progression. Tumor-associated macrophages, which are recruited to tumors by multiple growth factors and chemokines that are often produced by tumor cells,[8,36] induce the proliferation, survival, and invasion of tumor cells by producing a wide range of factors, including matrix metalloproteinases and growth factors such as fibroblast growth factor and epidermal growth factor.[37–39] A recent study by Neyen et al.[40] shows that tumor progression and metastasis are inhibited

TABLE 2 Tumor-infiltrating CD204-positive macrophage density in upper urinary tract cancer and patient outcomes (metastasis)

	Univariate analysis		Multivariate analysis			
	HR (95 % CI)	*p* value	HR (95 % CI)	*p* value	HR (95 % CI)	*p* value
CD204 (tumor center) (high vs. low)	4.78 (2.06–11.1)	0.0003	2.52 (1.02–6.22)	0.045	–	–
CD204 (tumor periphery) (high vs. low)	5.86 (2.40–14.3)	0.0001	–	–	3.10 (1.17–8.16)	0.022
Sex (female vs. male)	1.00 (0.46–2.17)	0.99	–	–	–	–
Age (≥70 vs. <70 years)	2.03 (1.00–4.12)	0.050	–	–	–	–
Side (right vs. left)	0.86 (0.43–1.72)	0.66	–	–	–	–
Tumor location (ureter vs. renal pelvis)	1.90 (0.95–3.80)	0.071	–	–	–	–
Tumor architecture (sessile vs. papillary)	1.57 (0.76–3.26)	0.23	–	–	–	–
Tumor grade (high vs. low)[a]	–	–	–	–	–	–
Lymphovascular invasion (present vs. absent)	6.73 (2.90–15.6)	<0.0001	2.79 (1.02–7.65)	0.046	3.03 (1.08–8.49)	0.035
Concomitant carcinoma in situ (present vs. absent)	3.16 (1.49–6.68)	0.0026	–	–	–	–
Tumor stage (pT2–pT4 vs. pTa–pT1)	9.84 (2.99–32.4)	0.0002	2.69 (0.64–11.4)	0.18	1.89 (0.41–8.80)	0.42
Lymph node metastasis (present vs. absent)	6.37 (3.13–12.9)	<0.0001	2.30 (1.07–4.94)	0.034	2.64 (1.25–5.55)	0.011
Adjuvant chemotherapy	2.87 (1.43–5.78)	0.0031	–	–	–	–

The multivariate Cox regression models initially included CD204 status (tumor center or periphery), gender, age at diagnosis, tumor side, tumor location, tumor architecture, tumor grade, lymphovascular invasion, concomitant carcinoma in situ, tumor stage, lymph node metastasis, and adjuvant chemotherapy. A backward elimination was performed with a threshold of $p = 0.05$; however, CD204 status, tumor stage, and lymph node metastasis were forced into the final models

CI confidence interval, *HR* hazard ratio

[a] Because patients with low-grade tumors did not experience an event, the hazard ratio could not be calculated

TABLE 3 Tumor-infiltrating CD204-positive macrophage density in upper urinary tract cancer and patient outcomes (cancer-specific mortality)

	Univariate analysis		Multivariate analysis			
	HR (95 % CI)	*p* value	HR (95 % CI)	*p* value	HR (95 % CI)	*p* value
CD204 (tumor center) (high vs. low)	5.41 (1.99–14.8)	0.001	2.75 (0.93–8.11)	0.067	–	–
CD204 (tumor periphery) (high vs. low)	5.19 (1.91–14.1)	0.001	–	–	2.50 (0.87–7.20)	0.089
Sex (female vs. male)	0.98 (0.39–2.50)	0.97	–	–	–	–
Age (≥70 vs. <70 years)	2.78 (1.19–6.52)	0.019	–	–	–	–
Side (right vs. left)	0.84 (0.37–1.91)	0.67	–	–	–	–
Tumor location (ureter vs. renal pelvis)	1.50 (0.66–3.44)	0.34	–	–	–	–
Tumor architecture (sessile vs. papillary)	2.15 (0.94–4.91)	0.069	–	–	–	–
Tumor grade (high vs. low)[a]	–	–	–	–	–	–
Lymphovascular invasion (present vs. absent)	13.4 (3.96–45.6)	<0.0001	5.15 (1.27–20.8)	0.022	5.24 (1.28–21.5)	0.022
Concomitant carcinoma in situ (present vs. absent)	3.30 (1.36–8.03)	0.0085	–	–	–	–
Tumor stage (pT2–pT4 vs. pTa–pT1)	22.7 (3.05–168.6)	0.0023	3.78 (0.38–37.7)	0.26	3.09 (0.28–33.7)	0.35
Lymph node metastasis (present vs. absent)	7.45 (3.26–17.0)	<0.0001	2.22 (0.92–5.35)	0.075	2.70 (1.15–6.32)	0.022
Adjuvant chemotherapy	3.63 (1.54–8.57)	0.0033	–	–	–	–

The multivariate Cox regression models initially included CD204 status (tumor center or periphery), gender, age at diagnosis, tumor side, tumor location, tumor architecture, tumor grade, lymphovascular invasion, concomitant carcinoma in situ, tumor stage, lymph node metastasis, and adjuvant chemotherapy. A backward elimination was performed with a threshold of $p = 0.05$; however, CD204 status, tumor stage, and lymph node metastasis were forced into the final models

CI confidence interval, *HR* hazard ratio

[a] Because patients with low-grade tumors did not experience an event, the hazard ratio could not be calculated

in CD204-knockout mice in two in vivo models of ovarian and pancreatic cancer. Moreover, treatment of tumor-bearing mice with 4F, a small peptide ligand of CD204 that competes with physiological CD204 ligands, inhibited tumor progression and metastasis.[40] Taken together, these observations suggest that tumor cells and $CD204^+$ macrophages may cooperate to contribute to more aggressive tumor behavior and that CD204 may be a potential drug

target in the prevention of metastatic cancer progression. Therefore, further studies on the crosstalk between urothelial cancer cells and $CD204^+$ macrophages are warranted.

Whereas $CD204^+$ cell density was associated with shorter metastasis-free and cancer-specific survival, it was not associated with bladder recurrence-free survival. It is likely that the ability of an upper urinary tract cancer to recur elsewhere in the urothelium may involve a different pathway. Whether other immune microenvironment markers such as lymphocyte surface antigens,[41–44] cytokines,[45,46] or chemokine receptors[45] can predict bladder recurrence is an important subject for future studies.

CONCLUSIONS

Tumor-infiltrating $CD204^+$ cell density significantly associated with adverse prognostic factors and shorter metastatic-free and cancer-specific survival in patients with upper urinary tract cancer. Although further studies are required to validate our findings, our results suggest that a specific immune microenvironment may be associated with biological behavior of urothelial cancer and that CD204 may serve as a novel prognostic biomarker for these tumors.

ACKNOWLEDGMENTS This work was supported in part by a research grant from the Ichiro Kanehara Foundation for the Promotion of Medical Sciences and Medical Care (Teppei Morikawa), and a Grant-in-Aid for Scientific Research (C) from the Japan Society for the Promotion of Science (Teppei Morikawa). We are grateful to Yumiko Nagano, Harumi Yamamura, and Kei Sakuma for excellent technical support.

CONFLICT OF INTEREST Takashi Ichimura, Teppei Morikawa, Taketo Kawai, Tohru Nakagawa, Hirokazu Matsushita, Kazuhiro Kakimi, Haruki Kume, Shumpei Ishikawa, Yukio Homma, and Masashi Fukayama declare no conflicts of interest.

REFERENCES

1. Albini A, Sporn MB. The tumour microenvironment as a target for chemoprevention. *Nat Rev Cancer.* 2007;7(2):139–147.
2. Wang T, Niki T, Goto A, et al. Hypoxia increases the motility of lung adenocarcinoma cell line A549 via activation of the epidermal growth factor receptor pathway. *Cancer Sci.* 2007;98(4):506–511.
3. Matsubara D, Morikawa T, Goto A, Nakajima J, Fukayama M, Niki T. Subepithelial myofibroblast in lung adenocarcinoma: a histological indicator of excellent prognosis. *Mod Pathol.* 2009;22(6):776–785.
4. Lu T, Gabrilovich DI. Molecular pathways: tumor-infiltrating myeloid cells and reactive oxygen species in regulation of tumor microenvironment. *Clin Cancer Res.* 2012;18(18):4877–4882.
5. Rahir G, Moser M. Tumor microenvironment and lymphocyte infiltration. *Cancer Immunol Immunother.* 2012;61(6):751–759.
6. Straussman R, Morikawa T, Shee K, et al. Tumour micro-environment elicits innate resistance to RAF inhibitors through HGF secretion. *Nature.* 2012;487(7408):500–504.
7. Lewis CE, Pollard JW. Distinct role of macrophages in different tumor microenvironments. *Cancer Res.* 2006;66(2):605–612.
8. Pollard JW. Tumour-educated macrophages promote tumour progression and metastasis. *Nat Rev Cancer.* 2004;4(1):71–78.
9. Komohara Y, Ohnishi K, Kuratsu J, Takeya M. Possible involvement of the M2 anti-inflammatory macrophage phenotype in growth of human gliomas. *J Pathol.* 2008;216(1):15–24.
10. Ohtaki Y, Ishii G, Nagai K, et al. Stromal macrophage expressing CD204 is associated with tumor aggressiveness in lung adenocarcinoma. *J Thorac Oncol.* 2010;5(10):1507–1515.
11. Kurahara H, Shinchi H, Mataki Y, et al. Significance of M2-polarized tumor-associated macrophage in pancreatic cancer. *J Surg Res.* 2011;167(2):e211–219.
12. Hirayama S, Ishii G, Nagai K, et al. Prognostic impact of CD204-positive macrophages in lung squamous cell carcinoma: possible contribution of Cd204-positive macrophages to the tumor-promoting microenvironment. *J Thorac Oncol.* 2012;7(12):1790–1797.
13. Ito M, Ishii G, Nagai K, Maeda R, Nakano Y, Ochiai A. Prognostic impact of cancer-associated stromal cells in patients with stage I lung adenocarcinoma. *Chest.* 2012;142(1):151–158.
14. Yoshikawa K, Mitsunaga S, Kinoshita T, et al. Impact of tumor-associated macrophages on invasive ductal carcinoma of the pancreas head. *Cancer Sci.* 2012;103(11):2012–2020.
15. Ino Y, Yamazaki-Itoh R, Shimada K, et al. Immune cell infiltration as an indicator of the immune microenvironment of pancreatic cancer. *Br J Cancer.* 2013;108(4):914–923.
16. Shigeoka M, Urakawa N, Nakamura T, et al. Tumor associated macrophage expressing CD204 is associated with tumor aggressiveness of esophageal squamous cell carcinoma. *Cancer Sci.* 2013;104(8):1112–1119.
17. Grignon DJ. The current classification of urothelial neoplasms. *Mod Pathol.* 2009;22 Suppl 2:S60–69.
18. Roupret M, Babjuk M, Comperat E, et al. European guidelines on upper tract urothelial carcinomas: 2013 update. *Eur Urol.* 2013;63(6):1059–1071.
19. Morikawa T, Hino R, Uozaki H, et al. Expression of ribonucleotide reductase M2 subunit in gastric cancer and effects of RRM2 inhibition in vitro. *Hum Pathol.* 2010;41(12):1742–1748.
20. Morikawa T, Sugiyama A, Kume H, et al. Identification of toll-like receptor 3 as a potential therapeutic target in clear cell renal cell carcinoma. *Clin Cancer Res.* 2007;13(19):5703–5709.
21. Braun M, Kirsten R, Rupp NJ, et al. Quantification of protein expression in cells and cellular subcompartments on immunohistochemical sections using a computer supported image analysis system. *Histol Histopathol.* 2013;28(5):605–610.
22. Miyata Y, Watanabe S, Kanetake H, Sakai H. Thrombospondin-1-derived 4N1 K peptide expression is negatively associated with malignant aggressiveness and prognosis in urothelial carcinoma of the upper urinary tract. *BMC Cancer.* 2012;12:372.
23. Takeda T, Kikuchi E, Mikami S, et al. Prognostic role of KiSS-1 and possibility of therapeutic modality of metastin, the final peptide of the KiSS-1 gene, in urothelial carcinoma. *Mol Cancer Ther.* 2012;11(4):853–863.
24. Liang PI, Li WM, Wang YH, et al. HuR cytoplasmic expression is associated with increased cyclin A expression and poor outcome with upper urinary tract urothelial carcinoma. *BMC Cancer.* 2012;12:611.
25. Miyazaki Y, Kosaka T, Mikami S, et al. The prognostic significance of vasohibin-1 expression in patients with upper urinary tract urothelial carcinoma. *Clin Cancer Res.* 2012;18(15):4145–4153.

26. Yoshimine S, Kikuchi E, Kosaka T, et al. Prognostic significance of Bcl-xL expression and efficacy of Bcl-xL targeting therapy in urothelial carcinoma. *Br J Cancer.* 2013;108(11):2312–2320.
27. Pignot G, Colin P, Zerbib M, et al. Influence of previous or synchronous bladder cancer on oncologic outcomes after radical nephroureterectomy for upper urinary tract urothelialcarcinoma. *Urol Oncol.* 2014;32(1):23.e1-8.
28. Kitamura H, Torigoe T, Hirohashi Y, et al. Prognostic impact of the expression of ALDH1 and SOX2 in urothelial cancer of the upper urinary tract. *Mod Pathol.* 2013;26(1):117–124.
29. Chromecki TF, Bensalah K, Remzi M, et al. Prognostic factors for upper urinary tract urothelial carcinoma. *Nat Rev Urol.* 2011;8(8):440–447.
30. Lughezzani G, Burger M, Margulis V, et al. Prognostic factors in upper urinary tract urothelial carcinomas: a comprehensive review of the current literature. *Eur Urol.* 2012;62(1):100–114.
31. Komohara Y, Hasita H, Ohnishi K, et al. Macrophage infiltration and its prognostic relevance in clear cell renal cell carcinoma. *Cancer Sci.* 2011;102(7):1424–1431.
32. Komohara Y, Horlad H, Ohnishi K, et al. M2 macrophage/microglial cells induce activation of Stat3 in primary central nervous system lymphoma. *J Clin Exp Hematop.* 2011;51(2):93–99.
33. Nonomura N, Takayama H, Kawashima A, et al. Decreased infiltration of macrophage scavenger receptor-positive cells in initial negative biopsy specimens is correlated with positive repeat biopsies of the prostate. *Cancer Sci.* 2010;101(6):1570–1573.
34. Ogino S, Galon J, Fuchs CS, Dranoff G. Cancer immunology: analysis of host and tumor factors for personalized medicine. *Nat Rev Clin Oncol.* 2011;8(12):711–719.
35. Galon J, Franck P, Marincola FM, et al. Cancer classification using the Immunoscore: a worldwide task force. *J Transl Med.* 2012;10(1):205.
36. Hagemann T, Wilson J, Burke F, et al. Ovarian cancer cells polarize macrophages toward a tumor-associated phenotype. *J Immunol.* 2006;176(8):5023–5032.
37. Wyckoff J, Wang W, Lin EY, et al. A paracrine loop between tumor cells and macrophages is required for tumor cell migration in mammary tumors. *Cancer Res.* 2004;64(19):7022–7029.
38. Mantovani A, Allavena P, Sica A, Balkwill F. Cancer-related inflammation. *Nature.* 2008;454(7203):436–444.
39. Qian BZ, Pollard JW. Macrophage diversity enhances tumor progression and metastasis. *Cell.* 2010;141(1):39–51.
40. Neyen C, Pluddemann A, Mukhopadhyay S, et al. Macrophage scavenger receptor a promotes tumor progression in murine models of ovarian and pancreatic cancer. *J Immunol.* 2013;190(7):3798–3805.
41. Gao Q, Zhou J, Wang XY, et al. Infiltrating memory/senescent T cell ratio predicts extrahepatic metastasis of hepatocellular carcinoma. *Ann Surg Oncol.* 2012;19(2):455–466.
42. Tsuchikawa T, Md MM, Yamamura Y, Shichinohe T, Hirano S, Kondo S. The immunological impact of neoadjuvant chemotherapy on the tumor microenvironment of esophageal squamous cell carcinoma. *Ann Surg Oncol.* 2012;19(5):1713–1719.
43. Katz SC, Bamboat ZM, Maker AV, et al. Regulatory T cell infiltration predicts outcome following resection of colorectal cancer liver metastases. *Ann Surg Oncol.* 2013;20(3):946–955.
44. Lee WS, Kang M, Baek JH, Lee JI, Ha SY. Clinical impact of tumor-infiltrating lymphocytes for survival in curatively resected stage IV colon cancer with isolated liver or lung metastasis. *Ann Surg Oncol.* 2013;20(2):697–702.
45. Yopp AC, Shia J, Butte JM, et al. CXCR4 expression predicts patient outcome and recurrence patterns after hepatic resection for colorectal liver metastases. *Ann Surg Oncol.* 2012;19 Suppl 3:S339–346.
46. Gu FM, Gao Q, Shi GM, et al. Intratumoral IL-17(+) cells and neutrophils show strong prognostic significance in intrahepatic cholangiocarcinoma. *Ann Surg Oncol.* 2012;19(8):2506–2514.

Anti-CCR4 mAb selectively depletes effector-type FoxP3$^+$CD4$^+$ regulatory T cells, evoking antitumor immune responses in humans

Daisuke Sugiyama[a], Hiroyoshi Nishikawa[a,1], Yuka Maeda[a], Megumi Nishioka[a,b], Atsushi Tanemura[b], Ichiro Katayama[b], Sachiko Ezoe[c], Yuzuru Kanakura[c], Eiichi Sato[d], Yasuo Fukumori[e], Julia Karbach[f], Elke Jäger[f], and Shimon Sakaguchi[a,1]

[a]Experimental Immunology, World Premier International Research Center, Immunology Frontier Research Center, [b]Department of Dermatology, and [c]Department of Hematology and Oncology, Graduate School of Medicine, Osaka University, Osaka 565-0871, Japan; [d]Department of Anatomic Pathology, Tokyo Medical University, Tokyo 160-8402, Japan; [e]The Third Section of Clinical Investigation, Kinki Blood Center, Osaka 536-8505, Japan; and [f]Department of Hematology and Oncology, Krankenhaus Nordwest, Frankfurt 60488, Germany

Contributed by Shimon Sakaguchi, September 23, 2013 (sent for review June 27, 2013)

CD4$^+$ Treg cells expressing the transcription factor FOXP3 (forkhead box P3) are abundant in tumor tissues and appear to hinder the induction of effective antitumor immunity. A substantial number of T cells, including Treg cells, in tumor tissues and peripheral blood express C-C chemokine receptor 4 (CCR4). Here we show that CCR4 was specifically expressed by a subset of terminally differentiated and most suppressive CD45RA$^-$FOXP3^{hi}CD4$^+$ Treg cells [designated effector Treg (eTreg) cells], but not by CD45RA$^+$FOXP3^{lo}CD4$^+$ naive Treg cells, in peripheral blood of healthy individuals and cancer patients. In melanoma tissues, CCR4$^+$ eTreg cells were predominant among tumor-infiltrating FOXP3$^+$ T cells and much higher in frequency compared with those in peripheral blood. With peripheral blood lymphocytes from healthy individuals and melanoma patients, ex vivo depletion of CCR4$^+$ T cells and subsequent in vitro stimulation of the depleted cell population with the cancer/testis antigen NY-ESO-1 efficiently induced NY-ESO-1–specific CD4$^+$ T cells. Nondepletion failed in the induction. The magnitude of the responses was comparable with total removal of FOXP3$^+$ Treg cells by CD25$^+$ T-cell depletion. CCR4$^+$ T-cell depletion also augmented in vitro induction of NY-ESO-1–specific CD8$^+$ T cells in melanoma patients. Furthermore, in vivo administration of anti-CCR4 mAb markedly reduced the eTreg-cell fraction and augmented NY-ESO-1–specific CD8$^+$ T-cell responses in an adult T-cell leukemia-lymphoma patient whose leukemic cells expressed NY-ESO-1. Collectively, these findings indicate that anti-CCR4 mAb treatment is instrumental for evoking and augmenting antitumor immunity in cancer patients by selectively depleting eTreg cells.

cancer immunotherapy | immunomodulation

Naturally occurring CD25$^+$CD4$^+$ regulatory T (Treg) cells expressing the transcription factor forkhead box P3 (FOXP3) are indispensable for the maintenance of immunological self-tolerance and homeostasis (1, 2). Given that most tumor-associated antigens are antigenically normal self-constituents (3–5), it is likely that natural FOXP3$^+$ Treg cells engaged in self-tolerance concurrently hinder immune surveillance against cancer in healthy individuals and also hamper the development of effective antitumor immunity in tumor-bearing patients. Indeed FOXP3$^+$CD25$^+$CD4$^+$ Treg cells are abundant in tumor tissues (6–10), and their depletion augments spontaneous and vaccine-induced antitumor immune responses in animal models (10, 11). In humans, increased numbers of FOXP3$^+$CD25$^+$CD4$^+$ Treg cells and, in particular, decreased ratios of CD8$^+$ T cells to FOXP3$^+$CD25$^+$CD4$^+$ Treg cells among tumor-infiltrating lymphocytes (TIL) are well correlated with poor prognosis in various types of cancers (6, 7, 10). Some clinical studies have shown the potential of depleting CD25-expressing lymphocytes to augment antitumor immune responses (12, 13); yet other similar studies failed to support the effects (10, 14, 15). Because activated effector T cells also express CD25, and their production of IL-2 is required for the expansion of CD8$^+$ cytotoxic lymphocytes, CD25-based cell depletion may reduce activated effector T cells as well, cancelling the effect of Treg-cell depletion to augment antitumor immunity (10). In addition, it has been demonstrated in animal models that depletion of Treg cells as a whole can trigger autoimmunity (1, 16, 17). Therefore, a current key issue is to determine how Treg cells can be controlled to evoke and enhance antitumor immunity without affecting effector T cells or eliciting deleterious autoimmunity.

Human FOXP3$^+$CD4$^+$ T cells are heterogenous in phenotype and function (2). These cells can be dissected into three subpopulations by the expression levels of FOXP3 and the cell-surface molecules CD45RA and CD25: (*i*) FOXP3^{hi}CD45RA$^-$CD25^{hi} cells, designated effector Treg (eTreg) cells, which are terminally differentiating and highly suppressive; (*ii*) FOXP3^{lo}CD45RA$^+$CD25^{lo} cells, designated naive Treg cells, which differentiate into eTreg cells upon antigenic stimulation; and (*iii*) FOXP3^{lo}CD45RA$^-$CD25^{lo} non-Treg cells, which do not possess suppressive activity but secrete proinflammatory cytokines (18). In principle, these distinct properties of FOXP3$^+$ T-cell subpopulations can be exploited to augment antitumor immunity without inducing autoimmunity, for example, by depleting a particular Treg-cell subpopulation rather than whole Foxp3$^+$-cell population. One of

Significance

Regulatory T (Treg) cells expressing the transcription factor FOXP3 play a critical role in suppressing antitumor immune responses. Here we found that, compared with peripheral blood T cells, tumor-infiltrating T cells contained a higher frequency of effector Tregs, which are defined as FOXP3^{hi} and CD45RA$^-$, terminally differentiated, and most suppressive. Effector Treg cells, but not FOXP3^{lo} and CD45RA$^+$ naïve Treg cells, predominantly expressed C-C chemokine receptor 4 (CCR4) in both cancer tissues and peripheral blood. In vivo or in vitro anti-CCR4 mAb treatment selectively depleted effector Treg cells and efficiently induced tumor-antigen-specific CD4$^+$ and CD8$^+$ T cells. Thus, cell-depleting anti-CCR4 mAb therapy is instrumental for evoking and enhancing tumor immunity in humans via selectively removing effector-type FOXP3$^+$ Treg cells.

Author contributions: H.N. and S.S. designed research; D.S., H.N., Y.M., E.S., and Y.F. performed research; M.N., A.T., I.K., S.E., Y.K., J.K., and E.J. contributed new reagents/analytic tools; D.S., H.N., Y.M., and S.S. analyzed data; D.S., H.N., Y.M., and S.S. wrote the paper; and M.N., A.T., I.K., S.E., Y.K., J.K., and E.J. collected clinical samples and data.

Conflict of interest statement: H.N. received a research grant from Kyowa Hakko Kirin Co., Ltd.

[1]To whom correspondence may be addressed. E-mail: nisihiro@ifrec.osaka-u.ac.jp or shimon@ifrec.osaka-u.ac.jp.

This article contains supporting information online at www.pnas.org/lookup/suppl/doi:10.1073/pnas.1316796110/-/DCSupplemental.

IMMUNOLOGY

the candidate molecules for such differential control of Treg-cell subpopulations is chemokine receptors, which allow Treg cells to migrate to a specific inflammation site via sensing specific chemokine milieu (19).

It has been shown that tumor-infiltrating macrophages and tumor cells produce the chemokine (C-C motif) ligand 22 (CCL22), which chemoattracts Treg cells as well as effector T cells expressing C-C chemokine receptor type 4 (CCR4) (6, 10, 20). In this report, we have addressed whether CCR4-targeting treatment is able to selectively reduce a particular Treg-cell subpopulation, rather than whole Treg population, and thereby elicit or augment in vitro and in vivo antitumor immune responses in humans.

Results

Depletion of CCR4$^+$ T Cells Predominantly Depletes eTreg Cells. In peripheral blood mononuclear cells (PBMCs) of healthy individuals, CCR4$^+$ T cells were present in both FOXP3$^+$ and FOXP3$^-$ T-cell fractions, and FOXP3^{hi} cells in particular were CCR4$^+$ (Fig. 1*A*). When FOXP3$^+$ T cells were classified into three populations by the levels of FOXP3 and CD45RA expression (18), FOXP3^{hi}CD45RA$^-$ eTreg cells (Fr. II) predominantly expressed CCR4 at the protein and mRNA level (Fig. 1*A*, and Figs. S1 and S2*A*). In contrast, FOXP3^{lo}CD45RA$^+$ naive Treg cells (Fr. I) scarcely expressed the molecule, whereas FOXP3^{lo}CD45RA$^-$ non-Treg cells (Fr. III) exhibited a moderate expression. Among FOXP3$^-$ cells, some CD45RA$^-$CD4$^+$ memory or activated T cells expressed CCR4, whereas CD45RA$^+$CD4$^+$ naive T cells did not. CD25 expression was well correlated with CCR4 expression with the highest CD25 expression by eTreg cells (Fr. II). Analyses of multiple samples of PBMCs from healthy individuals showed similar patterns of CCR4 expression by FOXP3 subsets (Fig. 1*B*). CD8$^+$ T cells, natural killer (NK) cells, CD14$^+$ monocytes/macrophages, dendritic cells, and B cells hardly expressed CCR4 at the protein and mRNA level (Fig. S2). In vitro depletion of CCR4$^+$ cells from PBMCs by magnet-bead sorting with anti-CCR4 mAb predominantly decreased CD4$^+$FOXP3^{hi}CD45RA$^-$ eTreg cells (Fr. II) and, to a lesser extent, CD4$^+$FOXP3^{lo}CD45RA$^-$ non-Treg cells (Fr. III), but spared CD4$^+$FOXP3^{lo}CD45RA$^+$ naive Treg cells (Fr. I) and FOXP3$^-$ cells (Fr. IV and V) (Fig. 1*C*). In contrast with anti-CCR4 mAb treatment, similar in vitro cell depletion with anti-CD25 mAb significantly reduced all of the FOXP3$^+$ subpopulations (Fr I, II, and III) and, to a lesser extent, FOXP3$^-$CD45RA$^-$CD4$^+$ activated or memory T cells (Fr. IV), with a relative increase in FOXP3$^-$CD45RA$^+$CD4$^+$ naive T cells (Fr. V) (Fig. 1*D*). PBMCs of melanoma patients showed similar patterns of CCR4 expression by FOXP3$^+$ subpopulations and similar changes in the composition of FOXP3$^+$ T-cell subsets after in vitro CCR4$^+$ T-cell depletion (Fig. S3).

Taking these data together, we find that CCR4 is predominantly expressed by eTreg cells and depletion of CCR4$^+$ cells results in selective reduction of eTreg cells, while preserving naive Treg cells and the majority of FOXP3$^-$CD4$^+$ T cells.

Tumor-Infiltrating Treg Cells Exhibit the eTreg-Cell Phenotype and Can Be Depleted in Vitro by Anti-CCR4 mAb. Although there is accumulating data that FOXP3$^+$ T cells predominantly infiltrate into tumor tissues (6, 7, 10, 21), their detailed phenotypes remain to be determined. Our analysis of TILs in nine melanoma samples revealed infiltration of a high percentage of CCR4$^+$ T cells, the majority of which were CD4$^+$FOXP3^{hi}CD45RA$^-$ eTreg cells (Fr. II), with only a small number of CD4$^+$FOXP3^{lo}CD45RA$^+$ naive Treg cells (Fr. I) (Fig. 2*A*). In vitro depletion of CCR4$^+$ T cells indeed dramatically reduced these tumor-infiltrating eTreg cells (Fig. 2*B*), indicating that anti-CCR4 mAb treatment is able to selectively deplete eTreg cells abundantly infiltrating into tumors.

In Vitro Induction of NY-ESO-1–Specific CD4$^+$ T Cells After CCR4$^+$ T-Cell Depletion from PBMCs of Healthy Donors and Melanoma Patients. With the efficient depletion of the eTreg-cell population by in vitro anti-CCR4 mAb treatment, we next examined

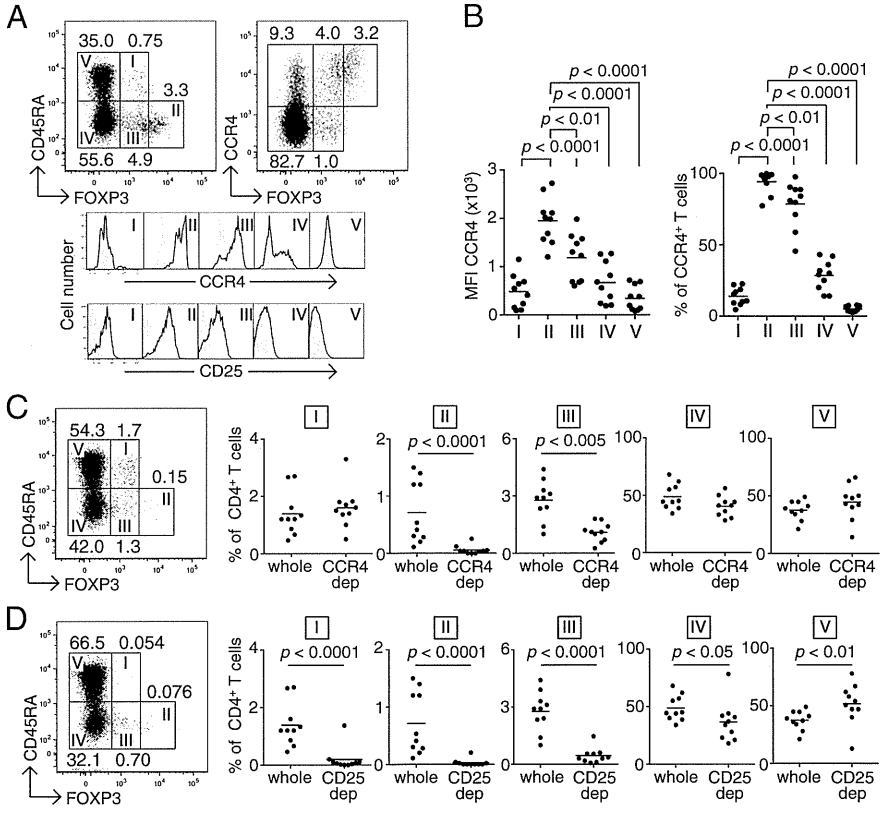

Fig. 1. Reduction of eTreg cells by in vitro depletion of CCR4-expressing T cells. (*A*) CCR4 and CD25 expression by subpopulations of FOXP3$^+$ Treg cells in PBMCs from healthy donors. CCR4 and CD25 expression levels were evaluated for each fraction. Representative data from 10 healthy donors are shown. (*B*) Median fluorescence intensity (MFI, *Left*) and frequency (*Right*) of CCR4 expression by each fraction of T cells in PBMCs of healthy donors (n =10). (*C*) Changes in the proportion of T-cell subpopulations after CCR4$^+$ T-cell depletion (CCR4 dep) (n = 10). (*D*) Changes in the proportion of T-cell subpopulations after CD25$^+$ T-cell depletion (CD25 dep) (n = 10). The numbers in *A*, *C*, and *D* indicate the percentage of gated CD4$^+$ T cells. Representative staining profiles in *A*, *C*, and *D* are from the same donor, and the same PBMC samples were analyzed in *B*–*D*.

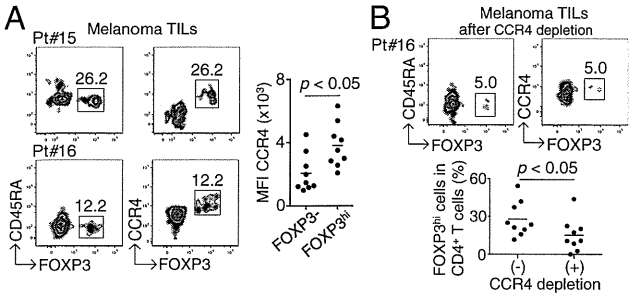

Fig. 2. Predominant infiltration of CCR4$^+$ eTreg cells into melanoma tissues. (*A*) CCR4 expression by melanoma-infiltrating T cells. CD4$^+$ T cells from melanoma sites were fractionated into subpopulations based on the expression of CCR4, CD45RA, and FOXP3; CCR4 expression by each fraction was analyzed. Data from two representative patients are shown. (*Right*) Summary of MFI of CCR4 expression by FOXP3$^-$ or FOXP3$^+$ cells (n = 9). (*B*) CCR4$^+$ CD4$^+$ T cells from melanoma tissues (Pt #16) were depleted of CCR4$^+$ T cells and then analyzed for the proportion of FOXP3^{hi} eTreg cells. (*Lower*) Percentages of FOXP3^{hi} cells among CD4$^+$ T cells after CCR4$^+$ cell depletion or nondepletion (n = 9). The numbers in *A* and *B* indicate the percentage of gated CD4$^+$ T cells.

whether CCR4$^+$ T-cell depletion from PBMCs of healthy donors was able to induce tumor antigen-specific CD4$^+$ T cells. We assessed specific T-cell responses to NY-ESO-1, a cancer/testis antigen, which is normally expressed by human germ-line cells and also by various types of cancer cells (4, 22). CCR4$^-$CD4$^+$ T cells or CD25$^-$CD4$^+$ T cells were cultured with CD4$^-$CD8$^-$ PBMCs as antigen-presenting cells (APCs), which were pulsed overnight with series of overlapping peptides covering the entire sequence of the NY-ESO-1 protein and X-irradiated (35 Gy) before use, as previously described (23, 24). Fifteen to 20 d later, NY-ESO-1–specific CD4$^+$ T cells secreting IFN-γ were enumerated by enzyme-linked immunospot (ELISpot) assay. Significant numbers of IFN-γ–secreting NY-ESO-1–specific CD4$^+$ T cells were induced in 7 of 16 healthy donors (43.8%), but only in the cultures with CCR4$^+$ or CD25$^+$ T-cell–depleted T cells (Fig. 3*A*, and summarized in Table S1). Furthermore, the frequencies of IFN-γ–secreting NY-ESO-1–specific CD4$^+$ T cells were higher after CCR4$^+$ T-cell depletion compared with CD25$^+$ T-cell depletion in five of seven healthy donors (71.4%) (Table S1). This result could be attributed in part to possible depletion of NY-ESO-1–specific CD25$^+$ activated T cells by anti-CD25 mAb treatment. The NY-ESO-1–specific CD4$^+$ T cells produced IFN-γ and TNF-α (Fig. 3*B*). Those cells induced in vitro after CCR4$^+$ T-cell depletion recognized NY-ESO-1 peptides at the concentration as low as 0.1 μM (Fig. 3*C*), and also NY-ESO-1 peptides produced by natural processing of the NY-ESO-1 protein by APCs, as previously shown with CD25$^+$ T-cell depletion (22, 24) (Fig. 3*D*).

We also attempted to determine whether Treg-cell depletion would evoke anti–NY-ESO-1 responses in apparently nonresponsive melanoma patients. With PBMCs from patients bearing NY-ESO-1–expressing melanomas, but without detectable NY-ESO-1–specific Ab in the sera, in vitro depletion of CCR4$^+$ or CD25$^+$ T cells and subsequent in vitro peptide stimulation induced IFN-γ– and TNF-α–secreting NY-ESO-1–specific CD4$^+$ T cells in three of eight patients (37.5%) (Fig. S4 *A* and *B* and Table S2). These NY-ESO-1–specific CD4$^+$ T cells appeared to express high-avidity T-cell receptors that recognized NY-ESO-1 peptides at a concentration as low as 0.1 μM, as seen with healthy donor T cells (Fig. S4*C*).

Thus, in healthy individuals as well as melanoma patients who had not raised spontaneous NY-ESO-1 immune responses, removal of eTreg cells by CCR4$^+$ T-cell depletion is able to efficiently induce high-avidity NY-ESO-1–specific CD4$^+$ T cells secreting effector cytokines.

CCR4$^+$ T-Cell Depletion Augments in Vitro Induction of NY-ESO-1–Specific CD8$^+$ T Cells from PBMCs of Melanoma Patients. PBMCs from melanoma patients were subjected to in vitro depletion with anti-CCR4 mAb or anti-CD25 mAb, and cultured with NY-ESO-1 peptide capable of binding to HLA class I of each patient. Seven to 10 d later, NY-ESO-1–specific CD8$^+$ T cells were detected by NY-ESO-1/HLA tetramers and analyzed for intracellular cytokine production. NY-ESO-1–specific CD8$^+$ T cells were induced in four of six patients (66.7%), and the responses were markedly augmented after depletion of CCR4$^+$ or CD25$^+$ cells (Fig. 4*A*). In addition, these NY-ESO-1–specific CD8$^+$ T cells recognized an HLA-matched malignant melanoma cell line and secreted IFN-γ and TNF-α (Fig. 4*B*). For example, Pt. #9 (HLA-A*02/29, B*44/27, C*03/04) harbored not only HLA-C*03–restricted NY-ESO-1–specific CD8$^+$ T-cells detected by HLA Cw*0304/NY-ESO-1 tetramers, but also those NY-ESO-1–specific CD8$^+$ T cells that recognized the SK-MEL 37 melanoma line (A*0201$^+$, NY-ESO-1$^+$) in an HLA-A2–restricted manner.

We also examined whether NY-ESO-1–specific CD8$^+$ T cells could be induced by directly adding mAb into cell cultures. Addition of anti-CD25 mAb or anti-CCR4 mAb reduced the frequency of CD4$^+$FOXP3^{hi}CD45RA$^-$ eTreg cells (Fr. II) (Fig. S5).

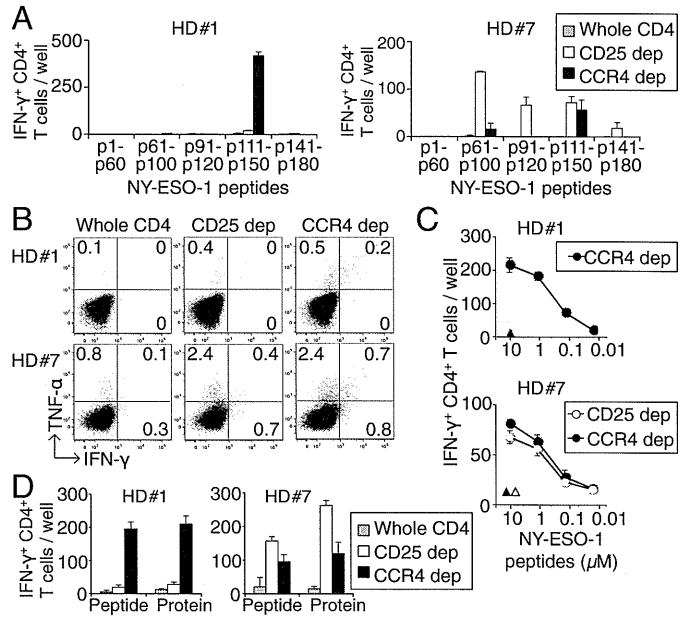

Fig. 3. Induction of cancer/testes antigen-specific CD4$^+$ T cells by depletion of CCR4- or CD25-expressing T cells in healthy donors. (*A*) CD4$^+$ T-cell responses to NY-ESO-1 peptides after depletion of CCR4$^+$ or CD25$^+$ T cells. CD4$^+$ T cells prepared from PBMCs of healthy donors were presensitized with APCs pulsed with NY-ESO-1 peptide covering the entire sequence of NY-ESO-1. Results of 2 (HD#1 and HD#7) among 16 healthy donors are shown. The numbers of IFN-γ–secreting CD4$^+$ T cells were assessed by ELISpot assay. (*B*) Intracellular cytokine secretion of CD4$^+$ T cells shown in *A*. The numbers in figures indicate the percentage of gated CD4$^+$ T cells. (*C*) Peptide dose-dependent recognition of NY-ESO-1–specific IFN-γ–secreting CD4$^+$ T cells. NY-ESO-1–specific CD4$^+$ T cells derived from CCR4$^+$ or CD25$^+$ T-cell–depleted cells (CCR4 dep and CD25 dep, respectively) were cultured with autologous activated T-cell APCs pulsed with graded amounts of NY-ESO-1 peptides and assessed for the number of IFN-γ–secreting cells as in *A*. Triangles indicate responses to control peptide at 10 μM. (*D*) Recognition of naturally processed NY-ESO-1 protein antigen by NY-ESO-1–specific CD4$^+$ T cells derived from whole CD4$^+$, CCR4$^+$ cell-depleted, or CD25$^+$ cell-depleted cells. NY-ESO-1–specific CD4$^+$ T cells from two healthy donors were cultured with autologous dendritic cells pulsed with NY-ESO-1 or control protein, or with NY-ESO-1 or control peptide. The experiments were independently performed twice with similar results.

IMMUNOLOGY